OCCASION

This publication has been made available to the public on the occasion of the 50th anniversary of the United Nations Industrial Development Organisation.

DISCLAIMER

FAIR USE POLICY

CONTACT

Please contact publications@unido.org for further information concerning UNIDO publications.

For more information about UNIDO, please visit us at www.unido.org

UNITED NATIONS INDUSTRIAL DEVELOPMENT ORGANIZATION
Vienna International Centre, P.O. Box 300, 1400 Vienna, Austria
Tel: (+43-1) 26026-0 · www.unido.org · unido@unido.org

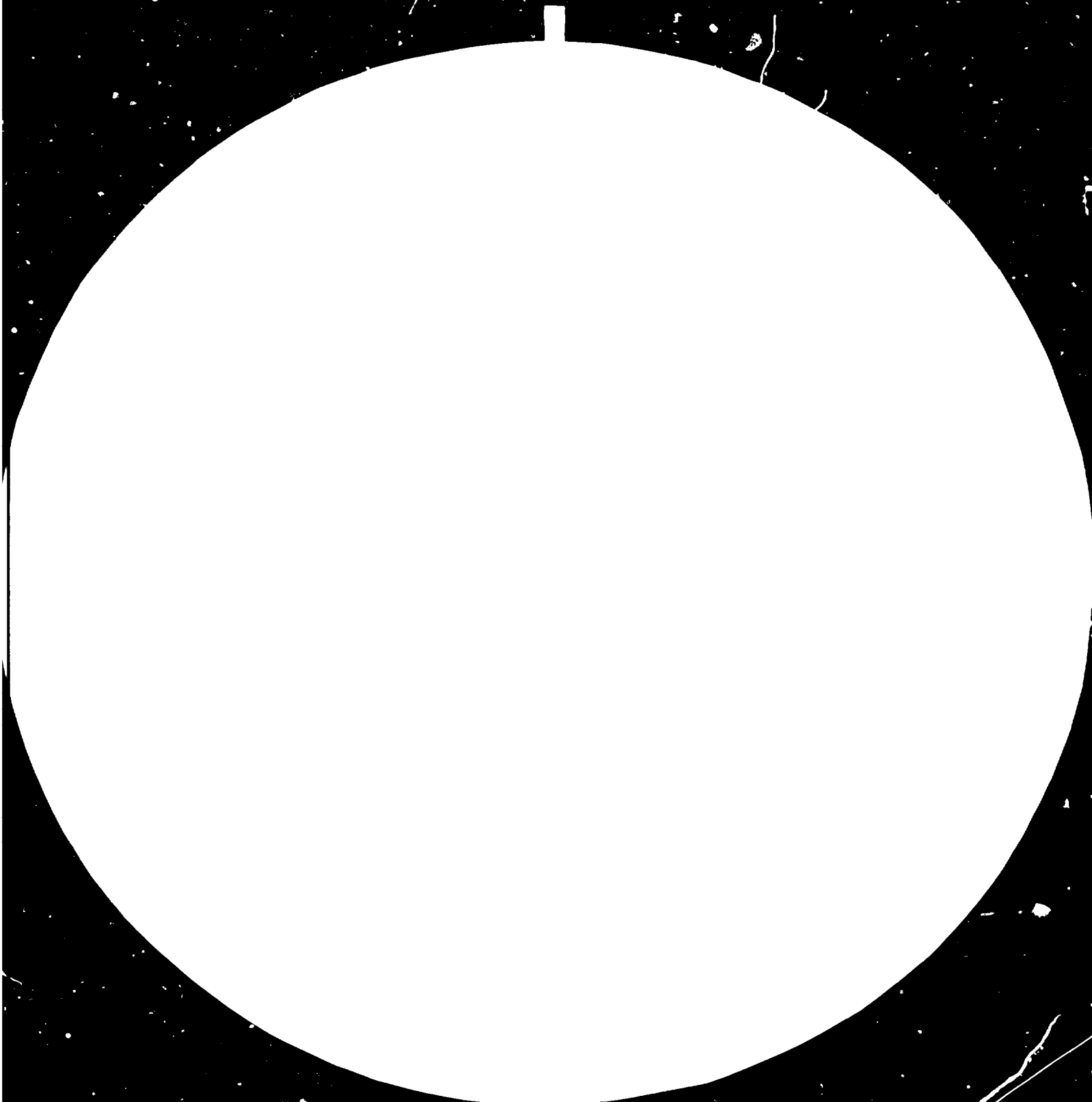

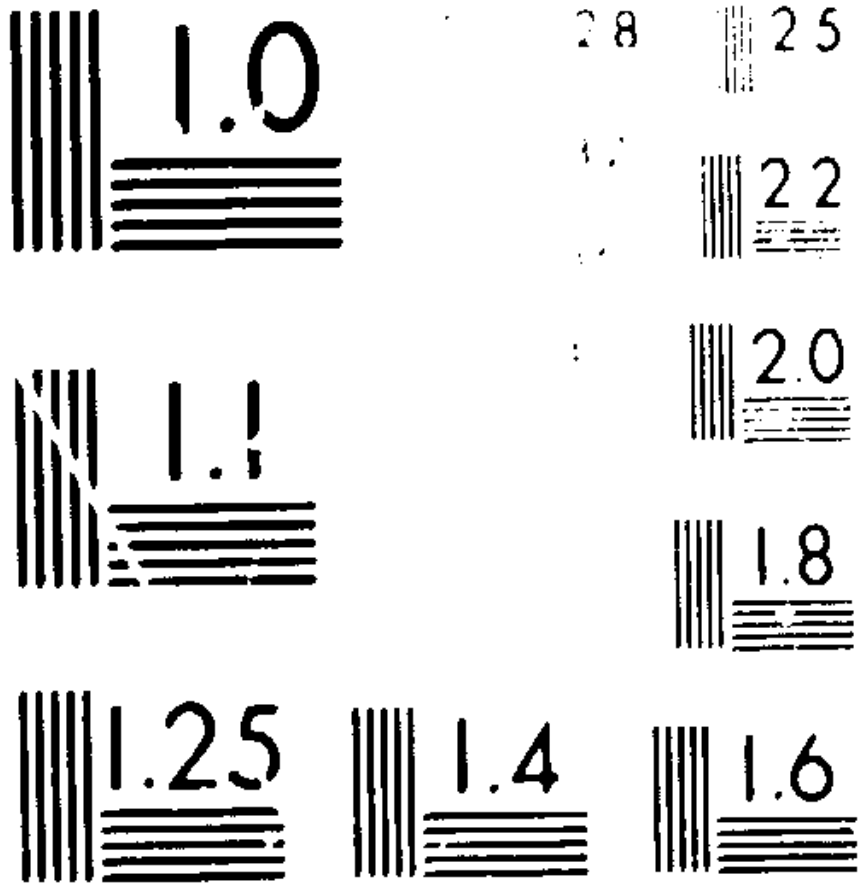
2.8
2.5
1.0
2.2
2.0
1.1
1.8
1.25
1.4
1.6

09495

United Nations Industrial Development Organization

GROUP TRAINING IN PRODUCTION OF ALUMINA VOLUME 5

PHYSICO-CHEMICAL CHARACTERISTICS AND ANALYSES OF BAUXITE, RED MUD, ALUMINA HYDRATE AND ALUMINA

ALUTERV-FKI

BUDAPEST, 1979

VOLUME 5

PHYSICO-CHEMICAL CHARACTERISTICS AND ANALYSES OF BAUXITE, RED MUD, ALUMINA HYDRATE AND ALUMINA

BY

Á. Csanády
A. Imre
Dr. M. Orbán

COLLABORATORS:
Á. Fehérváry
K. Ruhmann

Printed in
ALUTERV-FKI's Printing Shop
in 1979/1014

CONTENTS

FIGURES

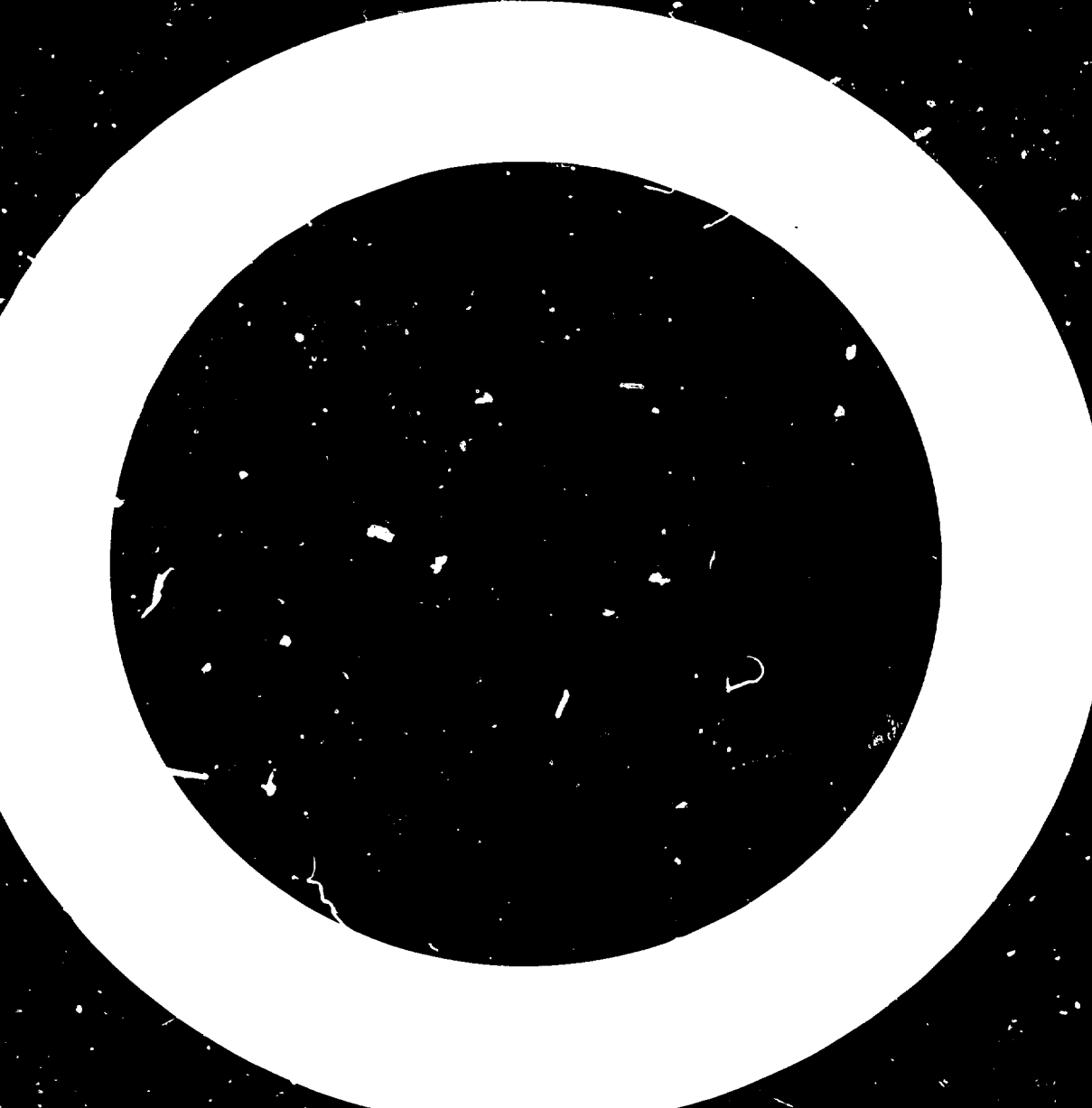

TABLES

INTRODUCTION

Apart from the chemical methods, physico-chemical and physical measuring figures are used for the qualification of raw-, intermediate- and final products of the alumina production process. This volume deals with the most important physico-chemical characteristics of the materials enlisted in the title, and the methods for their determination. In the course of description, the factors necessitating the determination of the given physico-chemical parameters and the reason of their measurement will be indicated briefly. Utilization possibilities of the informations derived from the measured parameters will be summarized, moreover, a short substantial comprehension of the references of the parameters' determination methods and the measuring processes used in the Hungarian alumina industry will be detailed, along with the reasons for selecting and using the latter.

Keeping in view the easier perspicuity, physico-chemical parameters and the fields of their utilization as detailed in this volume are collected in Table 5.1. As it can be seen in the Table, major part of the measuring figures is used for characterizing all the four qualified materials: therefore, to avoid repetitions, measurement techniques and the reference of the measurement methods are discussed in a separate chapter after the introduction. Methods of the Hungarian native alumina industry will be discussed more detailed than the others.

Physico-Chemical Parameters Used for the Qualification of Bauxite, Red Mud, Alumina Hydrate and Alumina

Table 5.1

Material tested	Physico-chemical parameters used for the characterization of the material tested
Bauxite	Grain-size and morphology
	Specific surface area
	Density
	Volumetric weight
	Porosity and distribution of pore volume
	Hardness
	Immersion heat
Red mud	Grain-size and morphology
	Specific surface area
	Density
	Porosity and distribution of pore volume
	Immersion heat
Alumina hydrate	Grain-size and morphology
	Specific surface area
	Density, apparent density
	Porosity and pore volume
	Heat transmission
	Immersion heat

Table 5.1 /cont./

Material tested	Physico-chemical parameters used for the characterization of the material tested
Alumina	Grain-size and morphology
	Specific surface area
	Density, apparent density
	Porosity and distribution of pore volume
	Heat transmission
	Fluorine-bounding capacity
	Angle of repose
	Dusting
	Rate of dissolution
	Immersion heat

DESCRIPTION OF PHYSICO-CHEMICAL TESTS, EQUALLY USED FOR THE QUALIFICATION OF BAUXITE, RED MUD, ALUMINA HYDRATE AND ALUMINA

SPECIFIC SURFACE AREA

The specific surface area is the size of the surface of a solid material by unit weight or unit volume. Its value can differ by orders of magnitude, in case of porous and nonporous materials, respectively.

In case of nonporous materials, the specific surface area is the sum of the "external" surface area of the grains, whereas in case of porous materials it is given by the sum of the grains' "external" and the pores' "internal" surface area. Comparing the two, the internal surface area is greater by orders of magnitude and consequently, the external surface area is almost negligible. As a consequence of the above mentioned the specific surface area /S_m/ of the pores is a function of the pores' size:

$$S_m = \int_{r_o}^{\infty} f/r/dr$$

where: r = radius of the pore

r_o = lower limit of the radius of the pore

Methods for determining the specific surface area of the dust particles are enlisted in Table 5.2.

As it can be seen in the Table the measuring methods can be classified into three main groups. Owing to their accuracy, reliability, easy automation possibility and relatively simple

Methods for the Determination of the Specific Surface Area

Table 5.2

Methods	Reference
1. Gas /steam/ adsorption methods	
a/ on the basis of weight	
static	1, 2, 3, 4
dynamic	5, 6, 7
b/ volumetric	
static	8, 9, 10, 11
dynamic	12, 13, 14, 15
2. Solution adsorption methods	
a/ fluid adsorption	16, 17, 18, 19
b/ paint adsorption	20, 21, 22, 23
c/ radioactive indication	24, 25, 26, 27
3. Different physical methods	
a/ emanation method	28, 29, 30
b/ porosimetry	2, 31, 32
c/ X-ray diffusion	33, 34, 35, 36
d/ gas permeability	37, 38, 39, 40
e/ microcalorimetry	41, 42, 43, 44
f/ capillar condensation	45, 46, 47, 48
g/ electric potential	25, 49, 50, 51
h/ conductivity	25, 52

techniques, the measuring methods of the first group are the extensively used ones. ALUTERV-FKI, too, performs the specific surface area measurements by gas-adsorption methods recognized by international standards /25, 53, 54/, therefore, and because of their significance and widespread usage, they will be discussed in more details. The study will be started by the discussion of the theory.

The Brunauer-Emmett-Teller Theory

Till the establishment of the Brunauer-Emmett-Teller theory, /designated hereinafter as BET theory/, no methods of adequate accuracy were known for measuring the specific surface area. Since the time it appeared, the BET adsorption isotherm equation and surface area determination method is the most commonly used system for this purpose /8/.

When deducing their equation, the authors assumed that first a layer of a single molecule's width will develop with continuous growth during the adsorption, followed by a multilayer covered stage and then by gas condensation /Fig. 5.1/.

In the practice, only the short form of their equation - suitable for the description of the total adsorption isotherm - is used for the surface determination:

$$\frac{V}{V/P_o - P/} = \frac{1}{V_m C} + \frac{C - 1}{V_m C} \cdot \frac{P}{P_o} \qquad /1/$$

where: V_m = amount of gas required for monomolecular layer formation

V = adsorbed gas-volume, calculated for normal conditions

P = equilibrium pressure of the adsorbed gas-layer

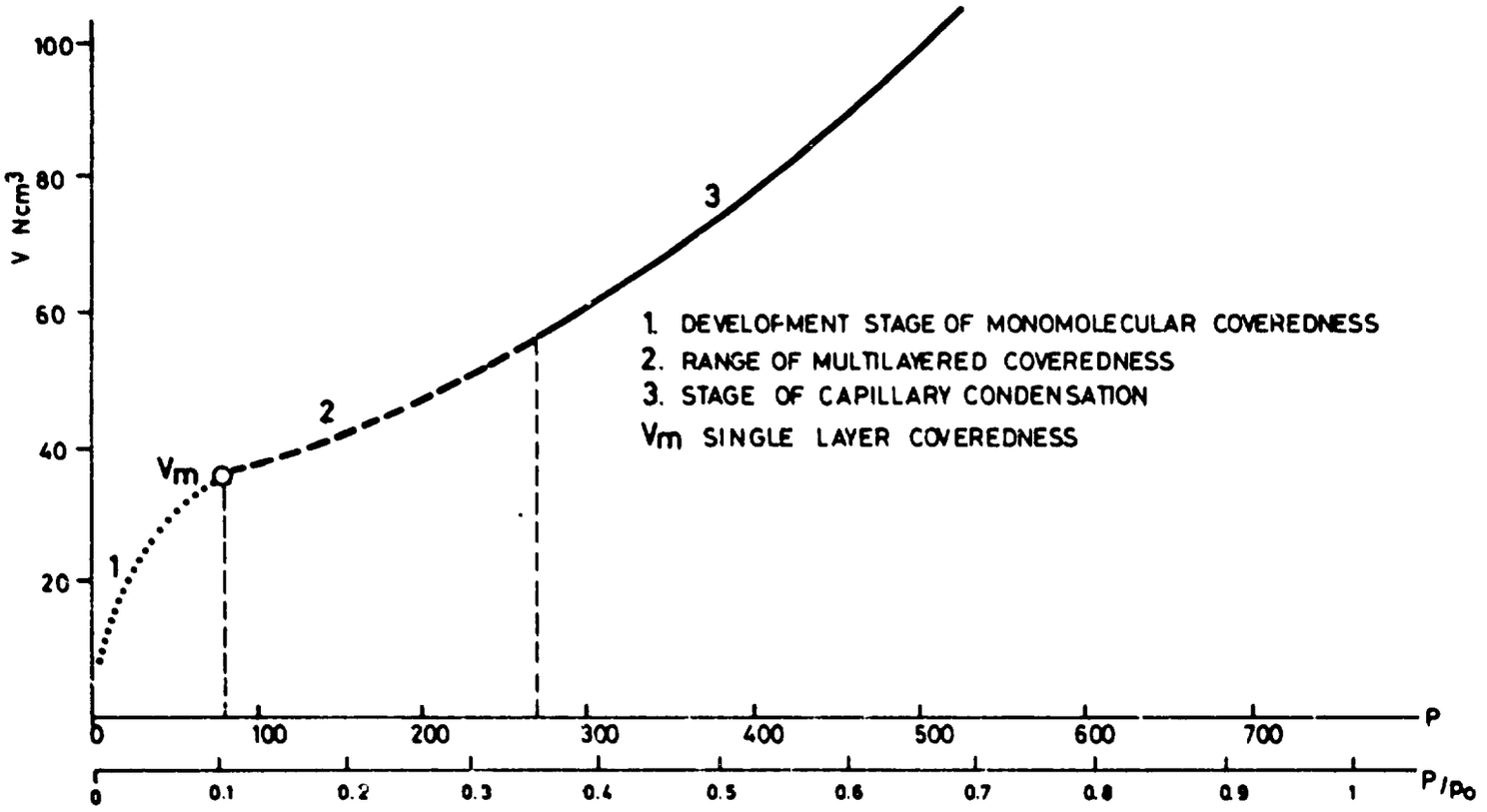

Fig. 5.1

NITROGEN ADSORPTION ISOTHERM OF THE Al_2O_3

P_o = saturated gas-pressure of the adsorbed gas, belonging to the given temperature

C = constant

Specific surface area is determined on the basis of V_m. For the determination of its value, V_m can be expressed from the equation /1/ or it can be graphically determined by using the above linear form. In this case the volumes V are plotted as P and P/Po, respectively; and the value of V_m is determined from the axial section and slope of the resulting straight line.

In equation /1/ the constant C is a number without dimension: in the first approach its value can be calculated by means of the following relationship /9/:

$$C = \exp. \frac{E_I - E_L}{R_o T} \qquad /2/$$

where: E_I = adsorption energy of the single layer

E_L = condensation energy of the adsorbed gas or steam

R_o = universal gas constant

The values of $E_I - E_L$, measured for 12 different materials /iron catalyzer, silica gel, copper catalyzer, iron-oxide, Al_2O_3, etc./ were nearly identical. All the 12 values were within the range of 840 $\pm$ 70 cal/mol /3520 $\pm$ 293 J/mol/ /9, 10/. The value of C, consequently, depends only slightly on the material quality. In case of the most frequently used nitrogen-adsorption calculations, the value of C = 240 is resulted /10, 11/.

The specific surface area /S_m/ is given from the value of V_m by the following relationship /9/:

$$S_m = \frac{S_o V_m}{W} \qquad /3/$$

where: W = weight of the measured-in adsorbent /g/

S_o = is a constant, it represents the surface requirement of 1 cm^3 normal condition gas, in case of monomolecular adsorption. Its dimension is m^2/m^3. Its value can be calculated from surface area requirement of the adsorbed molecules by using the following formula /9, 10, 11/:

$$S_{o1} = S_1 \cdot n \qquad /4/$$

where: n = the Loschmidt number

S_1 = surface area requirement of the gas molecule, calculated on the basis of the liquid state density

S_{o1} = surface area requirement of 1 cm^3 of normal condition gas, calculated on the basis of the liquid state density

Surface area requirement of the gas molecule /S_1/ according to Brunauer, can be calculated as follows /55/:

$$S_1 = 4 \cdot 0.866 \left[\frac{M}{4\sqrt{2} \cdot N \cdot \rho} \right]^{\frac{2}{3}} \quad cm^2 \qquad /5/$$

where: M = molar weight of the gas /or steam/

ρ_l = density of liquid state adsorbate
N = Avogadro number

Equation /1/ can be used for the majority of adsorbents: in the

$$\frac{P}{P_o} = 0.05 - 0.35,$$

and sometimes in the

$$\frac{P}{P_o} = 0.05 - 0.50$$

relative pressure range for determining the surface area, i.e. in the range preceding and following the shaping of the single molecule layer.

The most accurate determination of the specific surface area by the BET method can be done using the values measured on 4-5 points of the isotherm. The result of the three-point determination deviates from this value only slightly /56/. In case of large-series measurements the one-point method can also be used /2/.

Measuring units of the specific surface area were first used in the alumina industry when production of special aluminas was commenced. Since that time the most important qualification parameter of Al_2O_3 adsorbents, catalyst carriers, synthetic industry fillers and abrasives, is the size of their surface. During the 20-30 years that have passed since the introduction of surface measurement in the alumina industry, it proved to be evident that the informations gained by these measurements can variously be utilized in the industrial technology, and that they also provide significant data for the technological development.

POROSITY AND DISTRIBUTION OF PORE VOLUME

The relation between the pore volume /V_{pore}/ and the total volume /V_{total}/ of the porous material is called porosity /ε/.

$$\varepsilon = \frac{V_{pore}}{V_{total}}$$

The porosity can be calculated with best accuracy using volumes measured in helium and mercury. In this case V_{total} represents the volume measured in mercury, and V_{pore} is the difference of the volumes measured in mercury and helium.

The measuring unit of porosity gives informations only for the total volume of pores in a unit volume material. In case the dimensions and size distribution of the pores are also required, the pore size distribution function must also be determined /Fig. 5.2/. The function provides informations about the pore sizes and the frequency of the different size pores. These data serve as information for the accessibility of the so-called internal surface /surface area of the pores/, i.e. they will indicate the size of molecules able to penetrate into the pores.

Apart from this, the size of the pores and their size distribution is in relationship with the solidity, contraction, compressibility /58/, moreover, in case of fillers, with the grain-bounding characteristics of the binding material, too.

Determination Methods of Pore Size Distribution

Several measuring methods have been developed for the determination of the size distribution curve /58/. The most important measuring processes and the related literature are enlisted in Table 5.3.

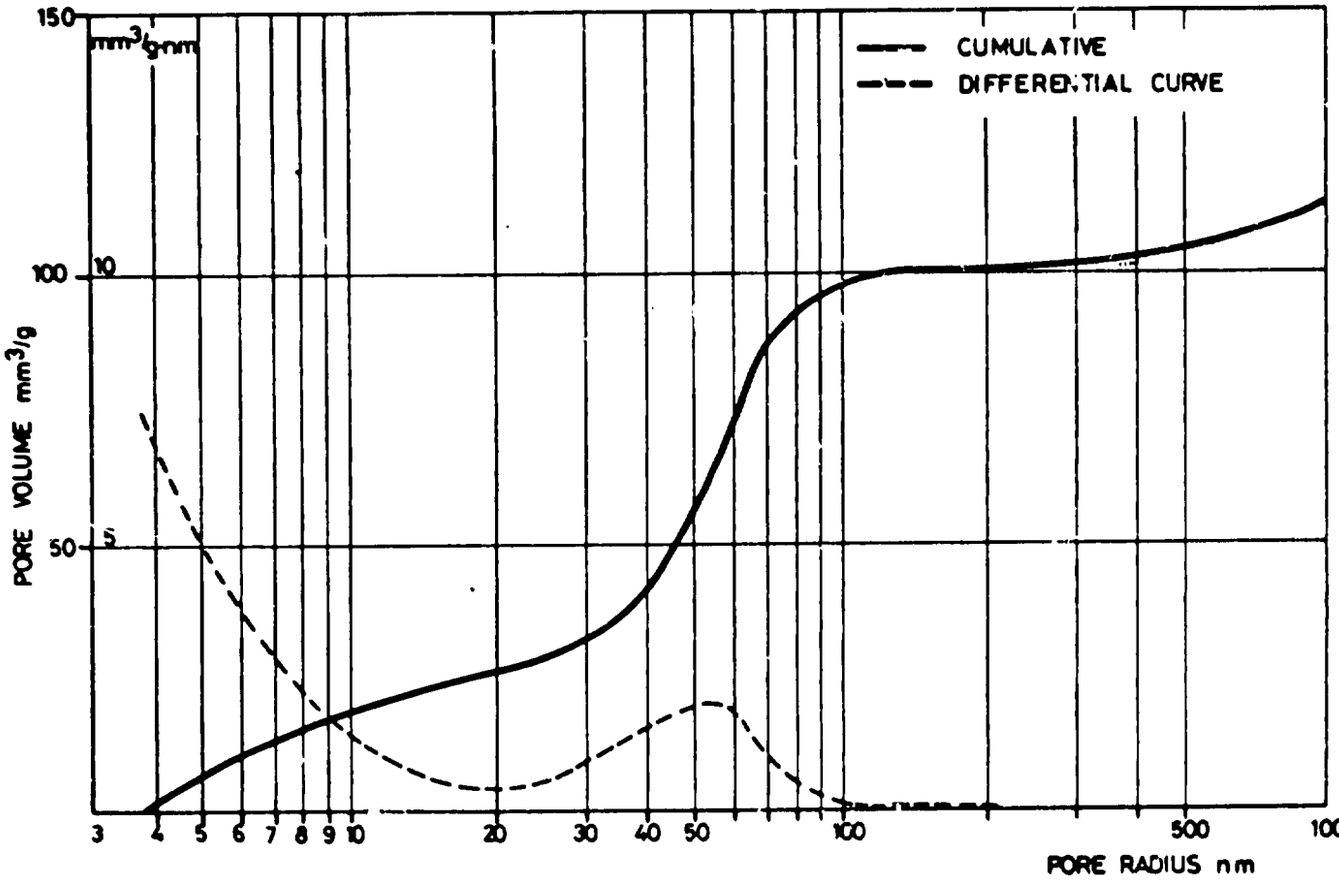

Fig. 5.2
CUMULATIVE PORE DISTRIBUTION AND FREQUENCY CURVE OF THE Al_2O_3 ADSORBENT

Most Important Methods of Determination of Porosity- and Pore Distribution

Table 5.3

Designation of the measuring method	Reference	Remarks
Density tests in Hg and helium	59, 60	Provides only the total pore volume or porosity, resp.
Optical microscopy	-	Measuring limit: 0.5 um. Provides the pore diameter and pore shape, but not the pore volume
Electron microscopy	61	Gives the pore diameter and pore shape
Gas-adsorption method with the help of adsorption and desorption isotherms	62, 63	Determination of pore volume and pore size distribution in the pore-range of r=1,4-30 nm
Mercury porosimetry	64, 65	Range of measuring: $r = 3\text{-}10^5$ nm
Small angle X-ray dispersion	66	Suitable to measure the pore distribution of materials containing pores of relatively homogeneous size distribution and of small diameter /20 nm/
Measurement of gas/steam sucking over velocity	67	Difficult to reproduce

As it cen be seen, density test provides only the pore volume. The optical microscopy does not give the pore volume besides the measuring range of the optical microscopy is not sufficient either for the determination of the total distribution. The X-ray dispersion method is applicable only in case of certain materials, and the measuring method of the sucking over velocity can only be used for comparative measurements of materials of the same type. As a result of the above, the gas-adsorption and mercury methods became widespread in the practice. The data of the two methods satisfactorily correspond to each other in the range of greater pore-sizes. In the size range of pores with radiants <10 nm, there can be a considerable deviation between the data gained by the two methods. Among others, the deformative effect of the high pressure mercury is mentioned as the reason of this deviation and, therefore, in the size range of <10 nm, data of the gas-adsorption method are considered to be more reliable. Owing to the above, the two measuring techniques practically complete each other.

Determination of Pore Size Distribution by Gas-Adsorption

In case the gas/steam isotherm on an adsorbent is determined by means of increasing and then decreasing series of pressures, the adsorption- and desorption isotherms of the given material will be obtained as a result. The relationship between the pore radii of the adsorbent and the equilibrium saturation steam pressure of the isotherms is described by the Kelvin equation /57/:

$$\lg \frac{P}{P_o} = - \frac{2 \sigma V}{rRT} \cdot \cos Q \qquad /7/$$

where: P = pressure of the adsorbate /gas/steam/

P_o = equilibrium steam pressure of the adsorbate at its boiling point temperature

τ = surface tension of the adsorbate, in liquid state

V = molar volume of the adsorbate = $\frac{M}{\varrho}$

M = molar weight of the adsorbate

ϱ = density of the adsorbate, in liquid state

r = pore-radius

R = universal gas constant

T = temperature /K^o/

Q = wettening contact angle

After expressing the value of "r" from the Kelvin equation, the pore-radius sizes belonging to the individual p-values of the isotherm can be calculated. With the help of these values and of the total pore spaces, the pore distribution function can be determined /Fig. 5.3/.

Determination of Pore Distribution by Mercury Porosimetry

Tests of gas-adsorption pore-size determination are mostly performed with nitrogen gas. The distribution function of the 1.5 - 30 nm pore-radius range can be determined with nitrogen /65-68/. Within the range of pores above this size, the tests are generally performed by mercury porosimeters /58, 65, 68, 69, 70/.

Mercury porosimetry is based on the realization that liquids having a wettening contact angle /Q/ on the given material greater than 90^o, can only intrude into the pores in case pressure is applied on them. The restrictive factor which must be suppressed by pressure is the surface tension of the liquid. Quantitative relationship between the radius /r/ and the pressure /P/ necessary to fill the capillary of the given dimension is described by the Washburn or Young-Laplace formula /58, 68, 69/:

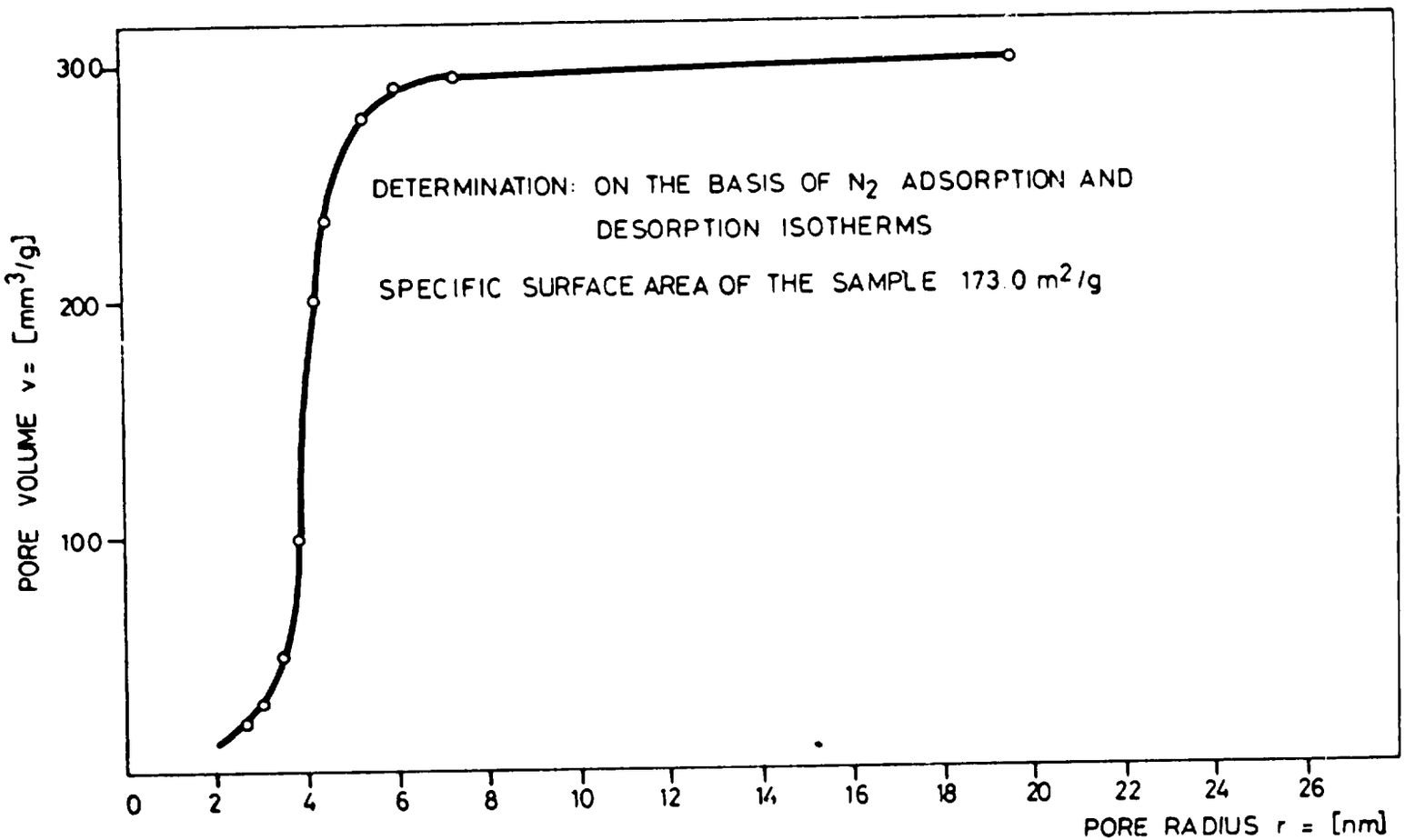

Fig. 5.3

CUMULATIVE PORE DISTRIBUTION CURVE OF BAYERITIC ALUMINIUM HYDROXIDE

$$Pr = 2 \sigma \cos Q$$

where: σ = surface tension of the liquid
Q = wettening contact angle of the liquid on the surface of the capillary

The pore distribution can be determined by the help of the formula, in case the amount of water intruding into the pores is determined in the function of the pressure /P/.

Distribution measurements are generally performed with mercury, as it does not moister the solid materials. The wettening peripheral angle of the mercury on different solid surfaces varies generally between 135-140°, consequently it changes only very slightly, thus in lack of the accurate measuring of the peripheral angle of the given material it is acceptable to calculate with average values. In most of the tests, the value of the peripheral angle is accepted to be 140°. The error of its value shows up in the number-value of the pore-radius, but it does not influence the shape of the distribution.

As for the accuracy of tests, the purity of the mercury is of high importance, as its contaminants considerably change the surface tension / σ /. Surface tension of the pure mercury is 480 din/cm /0.048 N/mm/ /69/. Calculating with Q = 140° and σ = 480 din/cm, and assuming that the pores are of cylindric shape, the relationship /8/ can be simplified to the following form /69/:

$$r = \frac{7500}{p} \quad nm \qquad /9/$$

With the help of the formula, the size of radius belonging to the individual pressure values can quickly be calculated, and the cumulative and frequency curves, respectively, can be constructed by the method described at the gas-adsorption system /Fig. 5.2 and 5.4/.

IMMERSION HEAT

The agglomeration and settling of dusts are affected to a high degree by their wettening characteristics /74/. The knowledge of red mud wettening characteristics, therefore, may provide important informations for the selection and setting of the optimum red mud settling.

Wettening of the solid materials is determined mostly by measuring the peripheral angle forming along the triple solid /liquid/ gas interface /74, 75/.

The peripheral angle can not be measured on dusts of such big size like the red mud is. In such a case the immersion heat gives information for the degree of wettening /74, 75, 76/. The immersion heat originates when immersing the tested dust into some liquid and, similarly to the peripheral angle, it gives information about the solid/liquid surface interaction:

$$q_i = h_{I/SL/} = \frac{\Delta H_I}{\Sigma} = h_{SL} - h_{So} \simeq e_{SL} - e_{So} = e_{I/SL/} \qquad /10/$$

where: $q_{i\Sigma}$ = immersion heat

= specific surface area of the solid material

ΔH_I = enthalpy change of the unit weight material

$h_{I/SL/}$ = enthalpy change of the unit surface

$h_{/SL/}$ = enthalpy of the unit solid/liquid interface

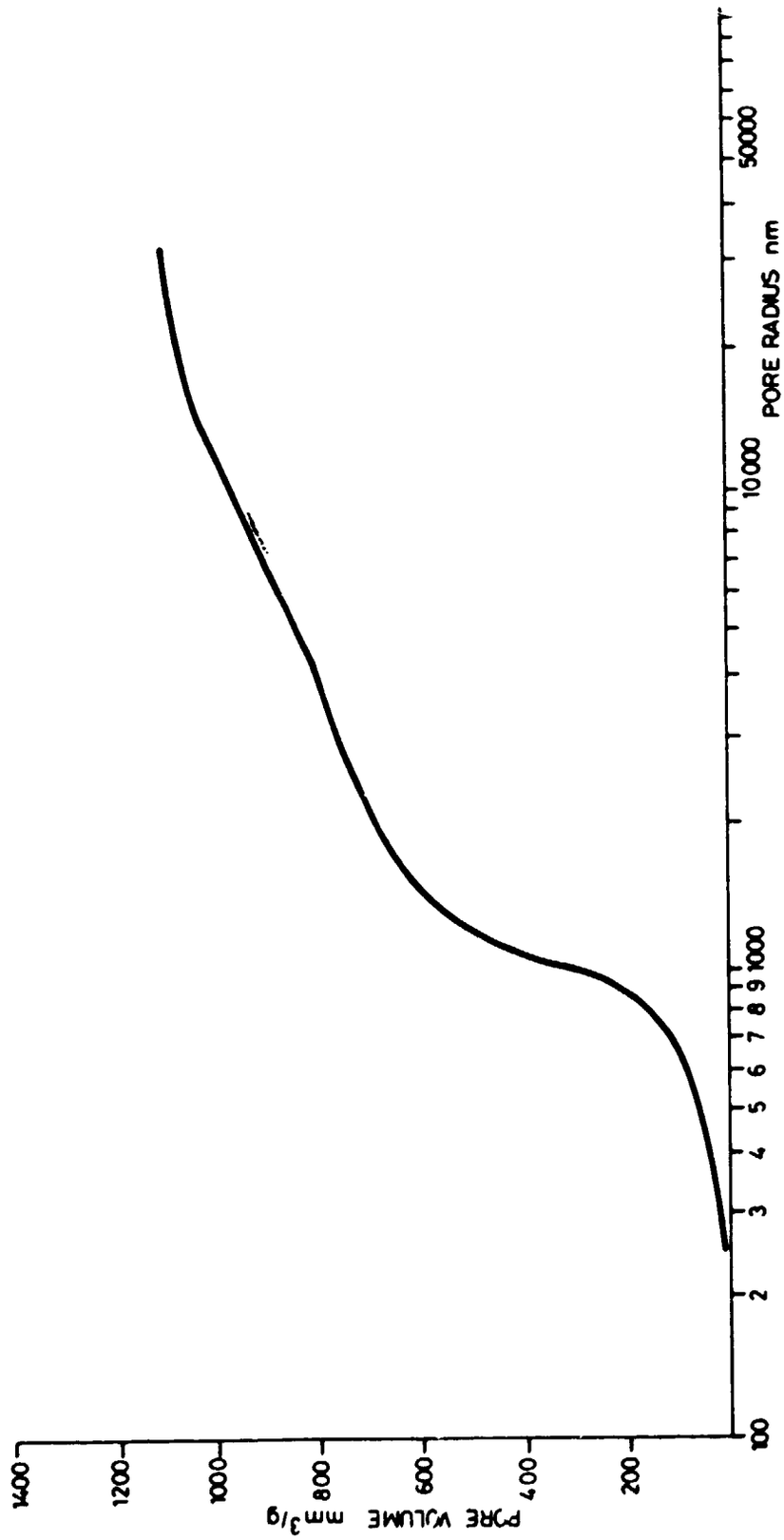

Fig. 5.4

CUMULATIVE PORE DISTRIBUTION CURVE OF PLANT ALUMINA

h_{Sc} = enthalpy of the unit solid/vacuum interface

$e_{I/SL/}$ = surface energy change of the unit surface

e_{SL} = surface energy of the unit solid/liquid interface

e_{So} = surface energy of the unit solid/vacuum interface

Consequently, the immersion heat is proportional to the change of enthalpy or owing to the negligible volumetric changes occurring during the wettening, to the change of the surface energy /75/.

The quantity of the immersion heat is determined by the interaction between the molecules of the solid material and those of the liquid. Its value, therefore, depends on the solid material/wettening liquid system. It is measured in semi-micro- or micro calorimeters so that the sample is put into an ampule before measuring it, the steams absorbed on its surface are removed in vacuum, then the ampule is sealed off and, being immersed in the calorimeter, it is crushed. After crushing, the rise of the temperature of the liquid is measured and on this basis the value of the immersion heat is calculated.

MORPHOLOGY

According to its original Greek interprepatation, morphology means study of the form. In a more general sense, it is a science dealing with the arrangement and connections of particles building the material. Taking this into consideration, by the word morphology are meant all spatial orders which are originated not by the relation of atomic points but by those of surfaces: from nm orders of magnitude, up to the range of visible dimensions.

The raw-, intermediate- and final products of the alumina production are all built up of grains. These individual

particles have a characteristic form and shape, and properties /morphology/ characteristic of their surface. During their formation, the above particles get into contact with each other and form, as regards physical and chemical aspects, reversible /agglomerate/ aggregations. The characteristics of the aggregations and their building particles considerably affect the alumina production processes /such as thickening, washing, precipitation, etc./: consequently, it is essential for the expert to get acquainted with their morphology.

Characteristics of the Morphology

Resulting from the above mentioned in order to possess scientific cognition of the morphology, synthetized data of several disciplines are required. Among these the most important informations generally used in the alumina industry are as follows:

- grain-size
- grain form and structure of the grain surface
- porosity and pore size distribution
- specific surface area

The measuring methods for the determination or recognition of the above are summarized below.

Measuring Methods of Cognition of Morphology

Determination of the Grain-Size

According to the special requirements, several methods were elaborated in order to determine the grain-size of the different materials. These methods can be divided into direct and indirect measuring processes. Table 5.4 gives a comprehension of the different methods.

Various Methods for the Determination of Grain-Size

Table 5.4

Method	Reference
Direct methods:	
Microscopy	/82, 84, 86, 87, 88, 90, 101, 104/
Electron microscopy	/71, 78, 79, 80/
Indirect methods:	
Electronic grain-counting method	/90, 95/
Methods based on the final settling velocity	/83, 84, 86, 87, 90, 91, 92, 93, 95, 98, 99, 100, 101, 102, 105, 106/

The methods and reference enlisted in Table 5.4 provide an opportunity to acquire informations of wider range, therefore, only methods used in the alumina industry and in our Institute will be descussed in detail.

Indirect Methods for Grain-Size Determination

Besides the grain-size, the microscopic processes discussed below give information about the shape of the grains, forms of the surface, pore sizes etc., too. Correspondingly, beyond size determination they are used for acquiring other informations, too.

Microscopy

The microscopic grain-size distribution determination methods are tests performed by optical- or electronic ray microscopes. Evaluation of the test can be done on the basis of indirect observations, microphotos and electronic calculation.

Measurements by optical microscope are performed within the range of 1-100 /um. The main objective of the test is the determination of the maximum grain-size.

Tests by electron ray microscopes are performed within the range of 0.01-5 /um. They are more accurate in this range than the optical microscopes. The electron ray, in fact, deeply penetrates into the material, and even the third dimension can be detected. The main purpose of the tests is the determination of the minimum grain-size.

Electron Microscopy

The two main fields of electron microscopy are used and described, respectively:

- Transmission electron microscopy, within this direct and indirect tests /77, 78/.
- Scanning electron microscopy: secondary electron operation mode, quantitative picture processing /79, 80/.

The Transmission Electron Microscopy

The transmission electron microscope utilizes the electron beam passing through a narrow substance for picture formation. The blown-up picture of the object is produced by projection, by an electron optic put in between the object and the screen. In case of such projection, the wave characteristics of the electron beam are utilized, and the effect inflicted by the object on the beam. It depends on the generation of the lenses,

whether the object itself or the characteristic diffraction diagram of its elementary structure is projected.

The electron optical contrast in the transmission electron microscope originates mainly on the basis of dispersion and diffraction phenomena. In case of indirect transmission tests, i.e. being performed by the replicas, the contrast formation is solely of topographical character. The electron beam falling at right angle onto the replica is of different orientation, as compared to the electron ray, but in amorphous layers of similar width it covers different distances. Since the dispersion is proportional to the atomic dispersion centres found in the direction of the beam, the difference in the width of the layers brings about intensity deviations behind the object.

In case of transmission tests of crystallic materials, the test based on the diffraction contrast is used most extensively. If electron ray passes through the crystal material put into the electron microscope, part of the incident radiation deviated on the grid plain assembly, and the other part goes on without any change of direction. Contrast effect between two image points can be experienced in case different deviation degrees exist on the object points corresponding to the image points.

The transmission electron microscopes were constructed in 1931 and have been used for routine material science purposes since the 40-ies. Electron microscopy of minerals is a new field of investigation at present. With the help of the instrument of increasingly better optical resolution - i.e. suitable to observe smaller structure units - new statements can be made on materials tested formerly. As regards bauxite, red mud, aluminium hydrates and aluminium-oxides, this means that the possiblities of cognition widened from the micromorphology towards the microstructure.

Scanning Electron Microscopy

The scanning electron microscope is one of the new types for structure analysing equipments generally applied at present. Since 1965 - the year it appeared in commercial trade - it provided a number of qualitative and, recently, quantitative informations about the structure, principally in the field of researches on the surface. The lighting system in this electron microscope is the electron source and the electron optics used as condenser. The resulting beam scans over a certain square-shaped area determined by the magnification. The beam is directed by the diverting coils built in before the two last so-called objective lens. The driving generator of these coils moves also the generator of the cathode ray tubes used for the reproduction of the picture. There are sensors built into the object space, in order to percept the originating signals. The signal percepted by the individual sensors is amplified by a wide-band amplifier and than it gets to the control grid of the monitoring cathode ray tube.

The electrons emerging from the surface layer of the sample being enlighted by the electron beam show characteristic energy distribution. Electrons of about 50 eV are originating from the surface layer of about 1-5 nm width. With the help of these secondary electrons, a given surface area of the material is looked at and the units built up of several atoms and the structure of their assembly, respectively, can directly be examined. The orientation of certain surface elements has a significant role in the contrast formation, the peaks and edges are in favoured position.

In case of echo-image operation, the scattered-back, high energy electrons are detected and they are used for picture formation. These electrons are originated already from the inside of the sample, i.e. from a few 100 nm's depth, and they help to get informations partly related to the topo-

graphy of the sample and partly to its chemical composition. The electrons also generate characteristic X-rays in the sample, typical of the elements in it. Microanalysers serve for the reproduction of the samples' element distribution structure. The echo-image operation, moreover, the microanalysis is very useful, sometimes indispensable completion of the secondary operation of scanning electron microscopy. Quantitative evaluation and statistical processing of the morphological informations of the scanning electron microscopic photos are carried out by picture analysers.

Determination of the Shape and Surface Structure of the Grains, Porosity and Pore Size Distribution

Informations concerning the shape of the grain and the condition of its surface are acquired by microscopic or electron microscopic tests mentioned. Microscopic photos provide data concerning the pore sizes and pore structure of the material, but in order to get accurate informations about them, in most cases, pore size determination methods based on other concepts as mentioned before are also utilized.

Determination of Specific Surface Area

The basic parameter of surface characteristics of materials with relatively high dispersity degree is the size of their surface. The size of the surface besides informations given about the degree of dispersity, porosity is a basic parameter of the determination of adsorption conditions, adsorption binding force, etc., too. The methods for its determination, utilization possibilities of its parameter are discussed in a previous paragraph. Here the only intention is to refer to the fact that the determination of the size of the surface provides significant informations for the morphology of the material as a whole.

GRAIN-SIZE DISTRIBUTION

Description of Grain-Size Distribution

A given industrial raw material or its ground product, is not built up of grains of the same size, but it is a mixture of grains with various forms and sizes, which can be best described by the so-called "grain-size distribution functions". The distributions can approximately be illustrated by the specific surface area, the corresponding average grain-size /grain diameter/ and the excessive values of grain-size distribution /81, 82, 83, 84, 85, 86/.

The determination of the above figures is rather difficult, since right at the beginning the question arises, what should be regarded, to be the standard main size of a grain /82, 83, 84, 86/. The answer depends on the type of measuring used /84, 86, 87/, consequently, systematization of the numerous measuring processes is regarded to be very significant and problematic.

Description of the System of Grain-Size Analyzing Methods

The first aspect of classifying the methods is whether the grain-size is determined by direct length measurement or by some indirect method /86, 87/.

Methods Based on Direct Grain-Size Measurement

There are two main methods for direct measurement of grain-size distribution: microscopic analysis and sieve analysis. Grains have generally three dimensions and out of those, their width is considered to be the standard /82, 84, 86/.

Microscopic Methods of Determining the Grain-Size Distribution

Microscopic methods of determining the grain-size distribution are tests performed by optical- or electron ray microscopes. Evaluation of the measurement can be carried out on the basis of: a/ direct observation, b/ microphotos and c/ electronic counting /80, 87, 88, 90, 103, 104/.

a/ Measurements by optical microscopes are performed in the range of 1 to 100 nm /86, 87, 90/. Under optimum conditions the accuracy of the test is $\sim \pm$ 5 per cent /absolute mean error/ /86, 90/. The relative inaccuracy is attributed to the fact that the smallest dimension of the grains can not be seen and, taking the smaller out of the two visible dimensions as overall or standard a considerable error occurs when calculating the grain-volume /especially in case of flat grains/, generally in positive direction /86/.
In general, the principal aim of optical measurements is to determine the maximum grain-size /86, 90/.

b/ Measurements by electron microscopes are performed in the range of 0.01 to 5 μm. They are more accurate in this range than the optical microscopes /86, 87, 90/. The electron ray, in fact, penetrates into the material to 5 to 10 μm depth and thus the third dimension can also be perceived. Above this dimension, however, it is an additional problem to draw conclusions based on the size distribution in the microsection plane of grinding of the embedded sample. The tests, however, can easily be automated /88/.
The main purpose of the measurement is to determine the minimum grain-size, which in some special cases, can be carried out to an order of magnitude of A°, using equipments of 1 A° resolution /86, 87, 88, 90/.

Direct Grain-Size Measurement by Sieve Analysis

Means of the analysis: screens of different apertures or sieve sets, where the apertures form geometrical progression. The most common is the sieve set of 2 quotient, based on geometrical considerations. The basis of the set is the so-called 200 mesh sieve /wire intersection/, having 0.075 mm apertures, according to the USA Tyler, ASTM E 11-61 or English BSS 410 standards. The mesh number of the European standards is different, in case of similar apertures: according to the German DIN 1171 and the Hungarian MSZ 695-59 standards, the 0.075 mm sieve is of 80 mesh. In case of the latter, the sieve aperture can be caiculated by the relationship d = 6/n, where: d represents the aperture and n the DIN sieve and the mesh, respectively /88, 84, 86, 90/.

In case of a geometrical sieve set, illustrating the analysis results vs. the logarythm of the sieve aperture /d/, the apertures corresponding to the subsequent sieves will be at the same distance from each other. This illustration method makes easy to construct the average diminution degree and its curve, the latter being, at the same time, the specific surface area curve, too /82, 83/.
It is a generally accepted fact for the determination of the characteristic grain-size that a grain /or class of grains/ can be characterized by the quadral screen aperture /side length of the square/ through which it can just fall. This intermediate main dimension, that is, the grain width will determine the through-fall /82, 83, 84/.

Operational principle of the sieve analyzers. The grain aggregate falls through the sieve only in case the grains are in relative motion, to the sieve panel. Moving the sieve panel brings about a relative motion of the grains. The mode of moving determines the application possibilities and the aspects of classification /86, 87, 90/. The grains can also

be moved by passing some medium through the apertures /86, 90/. This medium can either be water or air and, consequently, wet and dry sieve analysis methods can be mentioned.

The error of sieve analysis methods is generally between 1 to 1.5 per cent, in case the following measuring prescriptions are strictly kept /86, 87, 90, 91/:

a/ the amount of sample fixed in the standards must be taken out by normal averaging;
b/ the sample must be lump-free, that is, appropriately dry or satisfactorily dispergated;
c/ the intensity of the selected method should correspond to the solidity of the sample;
d/ the analysis time should carefully be chosen and the result of screening must be checked by check-screening;
e/ neither too much nor too few sieve classes are adequate;
f/ the error occurring in the mass weighing must be negligible relative to that of the screening;
g/ loss can not exceed 2 per cent.

Dry sieve analysis methods are suitable only for classifying well dried, not adherent materials. Apart from air-jet screening, these materials may not contain much fine grains /86, 87, 90/.

Manual methods of dry sieve analysis are suitable to screen coarse grain materials only. It is generally applied in case of screens having greater apertures than 5 mm /86, 87/.

The mechanical sieve analysing methods can be applied from mean to very fine distributions. The intensity of moving increases parallelly to the increase of the sample's fineness /86, 87, 90, 94, 95, 96/.

Shaken screens are moved horizontally. Aiming at increasing the intensity of screening, the sieve panel is being hit by a swinging mass, so that the screen would start to vibrate vertically, too. The method is suitable for screening mean size materials /86, 87, 90/.

Vibrating screens can be used for screening fine sized samples. The screen vibrates vertically with small amplitude and very high frequency /86, 87, 90/. Their special types are the so-called wobbler-screens, moving also in horizontal direction, and capable of screening to a lower limit of 60-100 /um, moreover, their sieve plate may be rubbed by a brush from below, in order to prevent filling /90/, /e.g.: ALLGAIER - Teumelsiebmachinen/.

Air-jet screens are the most effective dry sieve analyser units. They are generally used in a 500-10 /um range for high accuracy measurements /86, 87, 90, 95/. Sieves of 30-10 /um apertures are called microsieves: their diameter is very little /75 mm/ /96/. The principle of its operation is that the air-jet flowing in through a slot scans around the surface of the screen, throwing the sample continuously upwards. Grains of finer size than the apertures, when falling back, are carried by the air stream flowing downwards through the sieve plate to the dust filter or into the separator cyclone. Only one screen can be used at a time, therefore, the screening is performed in the so-called "negative screen order", starting with the finest screen, and measuring back the screen residues /e.g.: ALPINE A 200 LS type/.

Wet screen analysing methods are used for the analysis of finer and adhesive materials, or materials being originally wet. Its equipment generally correspond to those of dry screening /84, 86, 87, 91/.

Manual wet screen analysis. The screening is performed in negative order and, after separating the finest fraction, there may be a chance to switch over to the dry screening method. The sieve plate /frame/ is shaken vertically in a greater bowl of water, so that the water is flowing up-and-down through the apertures as long as all the fine grains leave the screen frame /86, 87/.

As regards the wet, mechanical screen analysing methods, the so-called under-water screening with shaken screen imitates the manual screening, but with mechanical drive whereas the vibration screening by rinsing utilizes water flowing from up-side down, aiming at promoting screening. In the latter method more screens are used simultaneously but, in case there are many grains of mud-size, rinsing-head frames are introduced even between the individual screens. Sieving can be performed with them to a lower limit of 25 /um. Ultrasonic sound-generated screening should separately be mentioned, it can be used with high intensity and almost without restraint to a lower limit of 5 /um /86, 87, 90, 95, 96/.

Methods Based on Indirect Grain-Size Determination

With regard to the great number of methods falling into this subject matter, the detailed description of all methods is disregarded herewith, only the methods used in the alumina industry or recommended for use will be described in more details.

Electronic Grain Counting Method

Its principle is based on the conductometry, and it transforms the size of the grains into analogue electric signs. The number and amount of signs is registered by an electronic unit, and it provides the measuring results in directly evaluated form /70, 75/. The unsatisfactory operational safety restricts its spreading.

Methods Based on the Final Velocity of Settling

Several methods and measuring units fall into this field, however, evaluation is always based on the Stokes' final velocity of grain settling, illustrated by the following formula:

$$V_o = -\frac{1}{18} \cdot \frac{\delta - \tau}{\eta} \cdot a \cdot d^2 \qquad / \text{cm/s} /$$

where: d = diameter of the equivalent sphere

δ = density of the sample /g/cm^3/

τ = density of the measuring medium /air or liquid/ /g/cm^3/

η = dynamic viscosity of the measuring unit /poise/

a = acceleration of the field /gravitational acceleration /g/ or acceleration of the centrifugal field $r \cdot \omega^2$ /cm/s^2/

In case of methods based on the final velocity of settling, instead of the actual grain-sizes the grains can be characterized by the so-called equivalent diameter of the little balls having the same settling velocity /and density/ as the grains have /83, 84, 86, 8 /. The deviation from the sphere-shape is characterized by a shape factor, which does not correspond to the numeric value used for the calculation of the specific surface area /86, 87, 91/. The measurement is possible due to the fact that even the finest grains attain their final settling velocity within a split second /86/.

Accuracy of the measurement: The sources of error vary related to the methods, the required dispersity and lack of air must be ensured in case working in liquid with the help of vacuum or wettening medium, respectively /86, 87, 91, 92, 105/.

Free /not hindered/ settling must be ensured in all methods /even in the air/, and this makes possible to measure in 0.5 volume per cent of sample /86, 87, 90, 93, 95/.

Sedimentation Methods

A main group of methods based on the settling velocity is characterized by the fact that the measuring medium is in standstill and only the grains settle in the measuring medium /in a liquid or in the air/, /86, 87, 90/.

Sedimentation in liquids is generally more accurate than in air, therefore, the former method is more widespread. The equipment of the traditional, old methods are very simple, but the up-to-date methods are significantly quicker and generally of automatic evaluation /86, 87, 90, 91, 93/.

Sedimentation methods in gravitational field in liquids can be applied in general in the 5 to 100 /um range and can be classified according to the method used to measure the variation of the density of suspension /86, 87, 90, 91/.

A/ Methods Reduced to Mass-Weighing

a/ Pipette methods /Köhn and Andreasen method/ can be characterized by the fact that only a small amount of sample related to the total amount is taken from a depth corresponding to the given settling way length /H_A/ for the determination of the concentration-change, from which the distribution can be determined:

$$s_D = \frac{c_o - c_t}{c_o} \cdot 100 \quad / \% / \quad \text{/cumulative residue curve/}$$

b/ The essence of decantation methods is the total amount of water above the H_A analysis depth is drained several /10 to 15/ times successively, and thus the total amount of sample is desintegrated to fractions on the basis of their settling velocity /86, 87, 90, 91, 93, 95/. The disadvantage of the methods is that they require a long time; this long duration can be reduced on the basis of the so-called "single decantation method" /106/. The primary distribution curve obtained on the basis of the single decantation is transformed by mathematical methods into the secondary cumulative curve which comes close to the real distribution. This method is the most accurate one, among the sedimentary methods /86, 106/.

c/ The sedimentation balances measure directly the amount of sedimented grains in a stationary medium. The principle of the evaluation of the measuring is similar, to the method of the single decantation /90, 100/.

B/ Methods reduced to density measurement measure the change of density in a given depth, for example by micromanometer or with the help of a floating object /86, 87, 91/.

C/ Methods Reduced to the Analysis of Light-Absorption Characteristics /Turbidimetry/

The method is based, from physical point of view, on measuring the light-absorbing ability of the suspensions. The light-absorbing ability depends on the number and size of grains floating in the suspension, that is, it is proportional to their specific surface area. Material characteristics have also importance, consequently, the equipment has to be calibrated for all types of new materials by a sedimentation method which can be reduced to mass weighing /86, 87, 90, 93, 101/.

In the course of the analysis the extinction /logarythm of absorbtion/ $E = \ln A = \ln /J/J_o/$ is measured instead of the absorption itself. J_o is the intensity of light passing through the pure measuring medium, whereas J represents the same passing through the suspension.

The relative mass of fractions can be calculated on the basis of the relation:

$$G_f = f_r \cdot r \cdot \Delta E$$

where: ΔE = change of extinction

r = radius of the equivalent sphere /calculated from the settling time/

f_r = the multiplying coefficient given in the function of r /determined by calibration measurement/

The final result, the mass proportion, can be calculated on the basis of the relation

$$S_1 = /G_{fi}/\Sigma\, G_{fi}/ \cdot 100$$

The evaluation became automatic recently, in to so-called scanning photometers, even the duration of the measurement is considerably shorter as compared to the traditional units and at the same time it is much more reliable /90/.

D/ Methods reduced to other radiation measurements are based on the absorption of X-ray and radioactive γ-radiation, moreover, on measuring the intensity of the generated secondary radiation. Apart from the deviation in the detect-

ing of the radiation intensity, the methods correspond, in principle, with the theories of photosedimentation /90/.

The measuring can be performed with satisfactory accuracy only in case if greater amounts are used: consequently, the SAMU unit of our Institute is used for settling analyses and not for the determination of distribution.

The purpose of tests performed in the centrifugal field is to reduce the analysis time and the sizes of the range of analysis of the grains. Measurements below 5 ,um are generally performed with centrifuge, to avoid long measuring time and below 2 ,um its usage is indispensable. The centrifuges can be used to a lower limit of $\sim$ 0.01 ,um, with a settling velocity increased to the 75,000-fold.

The variant of the simple decantation method elaborated for centrigufes, and reduced to mass weighing and density measurement can be mentioned here as an example. In the field of methods based on light-absorbing ability, the /Fritsch version of/ scanning photometer completed with centrifuge is mentioned.

Sedimentation in aeriform medium: its application reduces the analysis time, as even the fine grains settle relatively quickly in air. It is less accurate, works with 2-3 per cent error. A single variant, common in practice, can be mentioned here: the so-called Micromerograph, which operates similarly to the Sartorius sedimentation balance, and its basis is a 2 m long air-operated sedimentor tube.

Analysis /Classification/ by Flow-Stream Medium

The operation principle is that the gaseous or liquid medium flowing upwards /in opposite direction to the gravitational and centrifugal acceleration, resp. /with a velocity

corresponding to the settling velocity /v_t/ of grains with d_t diameter, carries all the finer grains of smaller settling velocity than /v_t/, and takes them out on the top of the equipment. The more quickly settling coarse grains pile up at the bottom. Their accuracy is similar to the former, i.e. 1-1.5 per cent, but they have the advantage of producing fractures out of the greater amount of samples which can be further analysed /chemical analysis, etc./ /82, 83, 84, 85, 86, 87, 90, 93, 95, 97, 98, 99/.

Silting-up methods utilize water as flowing medium /hydrometration/. The so-called hydrodynamic flow-units are used for this purpose /83, 84, 85, 86, 87/.

Silting-up can be performed in gravitational field by the so-called tubular flow-unit /Rheax or Koperecky-Krauss/ which produces two products, simultaneously. By series-connection of the tubes of different sizes all the fractions can be recovered at the same time /Mt Morgan multitube elutriator, Andrews kinetic elutriator, etc./. In due course, the most coarse fraction separates in the first tube /84, 85, 86, 87/.

Silting-up in a centrifugal field can be performed by the use of different drum centrigufes, the most approved type of which is the ALFA-LAVAL laboratory sedimentation separator /LAPX 202/, capable to operate both with reposing and flowing mediums /the former is adequate for sedimentation methods, too /85, 86, 87/.

The hydrocyclones are of intermediate type: not satisfactorily accurate in the research institutes, but still used in plants for automated analyses /91/.

Analysis /classification/ in a flowing aeriform medium. Generally air is used as a flowing medium /aerometration/. The units applied are the so-called aerodynamic flow-units and

air-elutriators, respectively. These are very quick and accurate methods, consequently they have become very widespread in the practice. The samples soaked in water can not be analysed by any other equipment operating with liquid /84, 85, 86, 87, 90, 97, 98, 99/.

a/ Classifying by Air-Stream in the Gravitational Field

The basic instruments are those of Gonell and Hollinger, respectively. They are long tubes where the air flows upwards from below. The fine grains leave the unit at its top and they are entrapped by a dust filter, the coarser grains are fluidized at the bottom, so that the possibly remaining fine grains could also get released. /The ALPINE 60 AN automatic analyser is produced in series./ They are used for analysis in the range of 10 to 50 μm, with $\pm$ 1-1.5 per cent error. Another variant of this basic type is the zi-zag classifier which eliminates the error caused by the grains' adhesion to the wall so, that the grains have to cross the air-flow repeatedly. The ALPINE MZM unit analyses within the range of 0.1 to 10 mm /84, 86, 90, 95, 98/.

b/ Classifying in Centrifugal Field, by Air-Stream

In order to extend the measuring limit, centrifugal field is used. One basic type has an impeller consisting of several revolving radial tubular pipes: the ALPINE 100 MZP type /90, 95, 98/, falls into this category, classifying within the range of 1 to 100 μm with $\pm$ 1 per cent accuracy.

In case of the other basic types, the slots in the impeller are not separated by radial walls, thus the air flows along spiral streamlines towards the centre /"upwards"/. The grain is affected by the resistance

of the medium and by the centrifugal acceleration in the opposite direction; in case of a d_t diameter, equilibrium state will occur, and these grains will move on a circular orbit. The smaller grains get into the central discharge, whereas the greater ones into the peripheral discharge unit /90/.

For the analysis of small amounts of laboratory samples, the so-called Bacho-Sichter unit is used /90, 99/. In case of 2.7 g/cm^3 density, within 4 to 30 μm interval, it operates with about 2 per cent accuracy. The ALPINE 132 MP unit /90, 95/, operated on the basis of the sample principle, but it requires 10 to 15 kg of sample, consequently it is only a semi-plant size unit. It analyses between the limits of 2 to 40 μm, with 1 per cent accuracy.

Application Fields of Determination of Grain-Size Distribution /86, 87/

a/ Determination of the grain-size composition of a given grain assembly.
b/ Determination of the amount of grains above or below the size limit, in raw material /in fractures/.
c/ Control of operation of classifying, crushing, grinding and dust-exhausting equipment.
d/ Determination of the desintegration degree.
e/ Production of determined-grade grains /fractions/ for further tests.

Analysis Results and Their Evaluation

The results of the tests give the mass quota or the cumulated mass quota related to the grain classes /81, 82, 83, 84, 86/.

The mass quota /m_i/ is the proportion of the mass of the fraction /q_i/, related to the total quantity measured-in /Q/, expressed generally in terms of percentage.

E.g.: $$m_i = q_i/Q$$

where: $Q = \sum_{i=1}^{2} q_i$, or in percentage form: $m_i = 100 \cdot q_i/Q$.

The relationships $\sum_{i=1}^{2} = 1$ or $\sum_{i=1}^{2} m_i = 100$ have to be true.

The grain-size class /or grain fraction, resp./ is an assembly of grains within a narrow size limit: the part remaining between two screens, or grains with a settling velocity falling in between the values corresponding to the two selected equivalent diameters.

1. Display of the Grain-Size Distribution

Display of the grain-size distribution can be made by tables, graphs or analytically in the form of a function /81, 82, 83, 84, 86/.

a/ Display by tables is very simple, only the size of the fractions and their mass quota have to be detailed in columns. The specification, however, can be started either with the largest or with the smallest sizes, in positive or negative order. Cumulating the mass quota in positive or negative order, the points of the so-called sieve residue curve or falling curve are resulted.

b/ Display by graphs: Plotting the calculated falling curve /s_F/ or the sieve residue curve /s_D/ /cumulated mass quota %/ into a linear co-ordinate system, vs. the grain-size /d/ in /um, the distribution function will result /this is a distribution function also in mathematical sense, $s_F = f/d/$ or $s_D = f/d/$ /.

The density function of the distribution function can also be constructed by graphic differentation, or by equalizing the underlying area of the so-called bar graph /81, 86/. The grain fraction limits must be plotted onto the abscissa, then vertical lines /parallel to the ordinate/ must be drawn from these points. Then the $g_i = \Delta S_i / \Delta d_i$ quotients have to be calculated, where: ΔS_i represents the mass quota of the fraction; Δd_i the difference or interval between the grain limits of the fraction. The bar graph of the density function is given by connecting the above vertical lines horizontally /parallelly to the abscisse/ at the height corresponding to the g_i frequency. Finally, drawing a continuous line instead of the bar-tops, on the basis of the equalized areas, the general form of the density function of the grain-size distribution function will be given. / $\Sigma g_i \cdot \Delta d_i = 1$ or 100 per cent./

c/ Analytic distribution functions can also be determined from the above results, based on the correlation calculation or on construction /81, 82, 83, 84, 85, 86/.

Four significant /that is, the most frequently used/ grain-size distribution functions will be mentioned, namely the Gaudin, the Rosin-Rammler, the normal and lognormal distribution functions.

Not all the constants and correlation coefficients of the four functions are calculated generally, but the test data are plotted in the diagram network corresponding to the individual functions, and that function is selected, in which the measured points approximate the best a straight line in the network. Then the constants of the given function are determined by the help of the correlation calculation. Most frequently the RR /Rosin-Rammler/ and the Log.Norm. /log-normal/ functions will be valid.

The Rosin-Rammler function is, in fact, a screen residue curve, and most frequently it is expressed as follows:

$$s_D = 100 \cdot e^{-\left(\frac{a}{d}\right)^b}$$

where: d = sieve opening and grain-size, resp.
a = constant /36.8 per cent grain-size/
b = constant /slope of the straight line in the RR-net/

The function is generally valid for finer ground materials, and since it is very easy to determine, and it can be related to other calculations, e.g. by the determination of the crushing energy requirement, it is the most important distribution function. The plotting of the function was standardized, and the a and b constants can be read off the standard RR-net directly, moreover, the product of the constant a and of the specific surface area, from which the specific surface area /cm^2/g/ /O_K/ can be derived by division.

The Kolmogorov lognormal distribution is valid, in fact, for every grain assemblies, thus it has great significance. Its disadvantage, however, is attributed to the relatively difficult formula, which is a falling curve. Its mathematical form is:

$$s_F = \frac{100}{d \cdot \sigma \cdot \sqrt{2\pi}} \int_0^d e^{-\frac{/\ln d - a/^2}{2\sigma^2}} d,$$

where: d = sieve opening and grain-size, resp.
a = constant /50 per cent grain-size/
σ = standard deviation

2. Calculation of the Specific Surface Area

The specific surface area can directly be calculated from the measuring results, and it is valid for grains approximating a sphere on the basis of the following relationship:

$$F_g = \sum_{i=1}^{l} F_i = \frac{6}{\delta} \cdot \sum_{i=1}^{l} \cdot \frac{S_i}{d_i}$$

where: S_i = direct mass quota of the fractions

d_i = average grain-size of the fractions:

$$\frac{d_j + d_{/j+1/}}{2} = d_i$$

δ = density of the sample

l = number of fractions

Shapes deviating from the spherical one are taken into account with the so-called "shape factor", which can be determined on the basis of the actual specific surface area measurement, for each the material type: /$A = F_{measured}/F_{calculated}$/. The more the shape of the grains deviated from the spherical one, the greater the "shape factor" will be /see Table 5.5/ /81, 83, 84, 86, 90/.

Shape Factor of Some Materials for Specific Surface Area Calculation

Table 5.5

Type of the material	Shape factor /A/
Spherical flue dust	1.22
Quartz	1.43
Powdered glass	1.90
Bauxite	1.80-2.10
Mica	9.27

Finally, the actual specific surface area will be: $F = A \cdot F_g$.

3. Average Grain-Size

Several average grain-size data can be calculated from the grain-size analysis data, e.g.: simple mathematical average, averages related to the cross section, volume, mass quota, specific surface area, etc., but only two calculation methods will be discussed in more details, because of their significance in the alumina industry /81, 82, 83, 86, 90/.

D_i in the formulae represents the average grain-size according to a certain principle; n_i is the number of grains in the fraction; d_i is the average grain-size of the fraction: $d_j + d_{/j+1/} : 2$. S_i is the mass quota /and volume quota, resp./ of the fractions; l is the number of fractions and A the shape factor.

a/ Average Weighed by the Mass Quota of the Screen Divisions

$$D_4 = \frac{\sum_{i=1}^{l} n_i \cdot d_i^4}{\sum_{i=1}^{l} n_i \cdot d_l^3} = \frac{\sum_{i=1}^{l} S_i \cdot d_i}{\sum_{i=1}^{l} S_i}$$

b/ Average based on the specific surface area: it is the most important average data in the crushing techniques and chemical industry /alumina industry/. It can be calculated from the grain-size analysis data according to the following:

$$D_F = \frac{100}{\sum_{i=1}^{l} \left(\frac{S_i}{d_i}\right)} \quad \text{or} \quad D_F = \frac{100}{A \cdot \sum_{i=1}^{l} \left(\frac{S_i}{d_i}\right)},$$

the latter is the more commonly used form.

From the analytically given grain-size function:

$$D_F = \frac{100}{A \cdot \int_0^{100} \frac{d_s}{d_i}}, \quad \text{where: } s = f/d/$$

The greatest problem of the calculation is the necessity to determine the minimum grain-size, which affects the numeric value of the specific surface area to the highest degree. The minimum size can generally be determined by electron ray microscopes.

PHYSICO-CHEMICAL TESTS OF BAUXITE

SPECIFIC SURFACE AREA OF BAUXITES

The specific surface area of bauxites depends on its quality, on the deposit, its geological antecedents, composition /such as the amount and quality of iron-containing constituents/, mineral composition, etc. A generally acceptable relationship is that the specific surface area of red mud produced form the bauxite comes near to that of the bauxite. In the majority of cases the surface area of red mud exceeds by 10-40 per cent that of bauxite. The specific surface areas of some bauxites are compiled in Table 5.6.

POROSITY AND PORE DISTRIBUTION OF BAUXITES

The cumulative pore size distribution curve and the frequency curve constructed from it by differentiation provides informations about the amount and size of pores in the analysed bauxite.

Bauxite is, in most cases, a raw material of high porosity. Its pore size distribution considerably depends on the place of its deposition and on the antecedents of the deposit /71/ /Fig. 5.5/. Similarly to other materials its degree of porosity and pore size distribution is related to its specific surface area /Fig. 5.5/.

Specific Surface Area of Bauxites

Table 5.6

Place of origin		Specific surface area m^2/g
-	Haiti	39.5 ± 1.9
Spinazzola	Italy	37.6 ± 0.6
Weipa	Australia	21.9 ± 2.7
Halimba	Hungary	12.0 ± 2.2
Mozanques	Africa	11.0 ± 3.1
Campo-Felice	Italy	10.3 ± 5.3
Chatchidika	Greece	2.4 ± 1.2
Fria	Africa	2.3 ± 2.0

It can generally be stated that the porosity of bauxite increases parallelly with the increase of the specific surface area. The porosity increases slightly during the processing of the bauxite. The total pore volume of unit weight red mud exceeds that of the bauxite by 10-30 per cent. The shape of the pore size distribution curve of the bauxite can be used for characterizing the red mud produced from it: consequently, knowing the bauxite's pore size distribution, conclusion can be drawn on the pore size distribution of its red mud. This relationship is illustrated in Fig. 5.6.

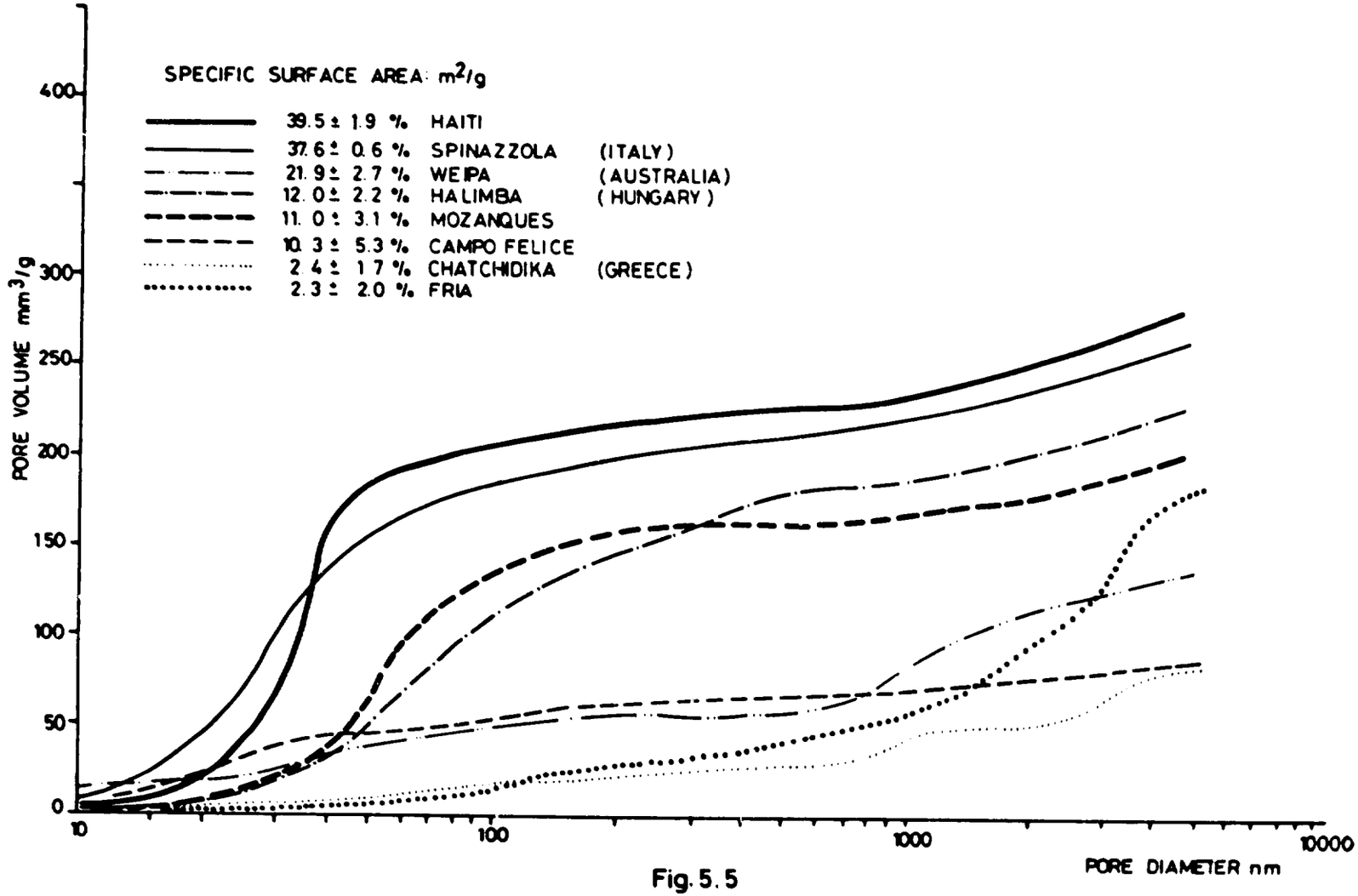

Fig. 5.5
PORE SIZE DISTRIBUTION OF BAUXITE

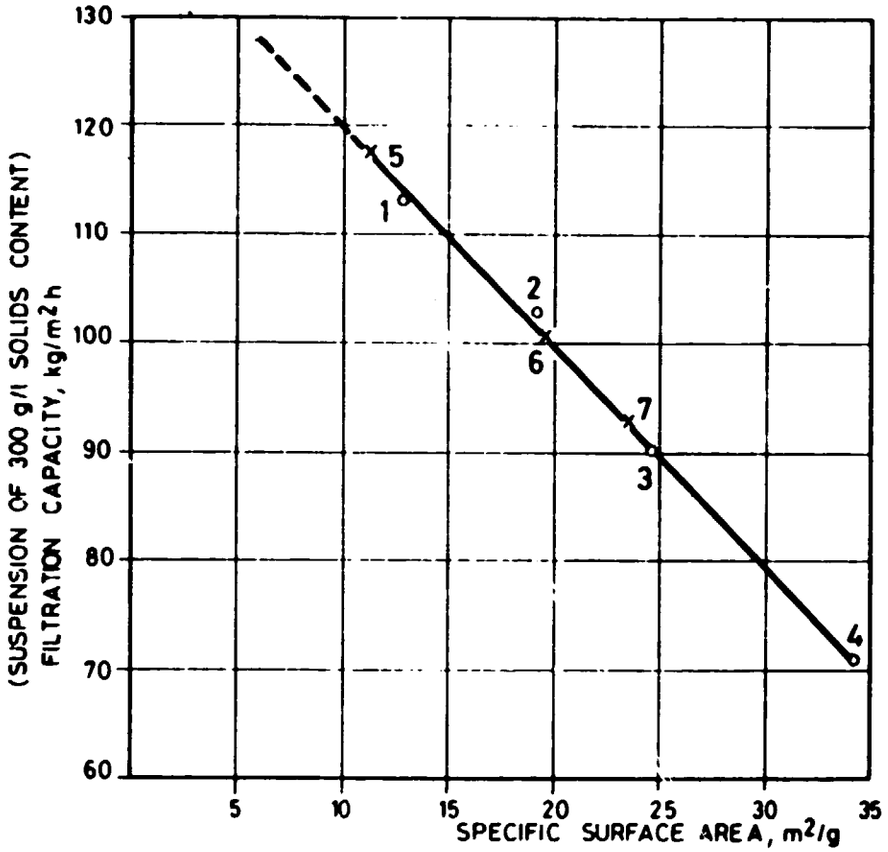

1. HEMATITIC MUD OF THE ISZKASZENTGYÖRGY BAUXITE
2. HEMATITIC GOETHITIC MUD OF THE HALIMBA BAUXITE
3. GOETHITIC MUD OF THE ISZKASZENTGYORGY BAUXITE
4. MUD OF THE DOLOMITIC HALIMBA BAUXITE

5-7. MUD OF THE OBROVAC BAUXITE

Fig. 5.6

FILTRATION CAPACITY OF RED MUDS IN THE FUNCTION OF THE SPECIFIC SURFACE AREA

IMMERSION HEAT OF BAUXITE

The order of magnitude of the bauxites' immersion heat is illustrated on the basis of two Hungarian bauxites in Table 5.7.

Immersion Heat of Bauxite

Table 5.7

Denomination of the material	Immersion heat Joule/m^2
Halimba bauxite, Hungary	0.693
Dolomite bauxite of Halimba, Hungary	0.365
Red mud of the Halimba bauxite, Hungary	0.570
Red mud of the dolomite Halimba bauxite, Hungary	0.760

The value of the immersion heat for bauxite is generally 0 to 1 Joule/m^2, indicating that it is a material of high surface energy. Immersion heat of red mud produced of the bauxite is principally the function of the bauxite's phase composition and, of the immersion heat of the materials forming from them.

MORPHOLOGY AND GRAIN-SIZE OF BAUXITE

In case of the bauxite types, the grain-size and the morphology is discussed together, because of practical purposes. The detailed analysis of individual mineral grains constituting the bauxites /107, 108, 109, 110/ started only when the scanning electron microscopes were introduced. Formerly the mineral components were tested by transmission electron microscopes /111/. It was stated that the individual mineral grains of most bauxites are smaller than 1 /um: the size of crystallites of the Hungarian bauxites, for instance, is generally between 0.1 to 0.3 /um /112/. Although few systhematical data are known only, it is obvious that the degree of crystallization, size and morphology of the individual mineral grains is not negligible as regards the technological processing /113/.

Besides others mainly geological factors, the space filling possibilities of bauxite are determined by the above parameters of individual crystallites. In most of the bauxites the individual crystallites coalesce into smaller or greater assemblies and these assemblies as structural elements build up the bauxites. From petrographical points of view, the space filling which can be analysed by the electron microscope provides more informations, than the so-called porosity, that is, the percentage ratio of the filled and unfilled space /114/. The size and shape of the unfilled spaces in the bauxites, however, can vary considerably, independently of the fact whether the percentage of porosity is small or great. Bárdossy, Csanády and Csordás described the systhematic morphological analysis of bauxites of different age and geographical origin /115/. Their conclusions will be summarized below.

Quaternary karstic bauxites have the smallest /50-200 nm/, certain laterite bauxites of high terrain situation the greatest /100,000-500,000 nm/ grain-size. The grain-size of karstic bauxites without overburden is generally smaller by one order

of magnitude at least than that of the laterite bauxites. The reason of this difference is explained by the physical-chemical effects of the carbonate surroundings hindering the crystal growth.

Generally, the smaller the grain-size of a bauxite mineral is the more irregular the shape and surface of its grains are. On the basis of X-ray and infra red adsorption analyses, the same refers to its crystal structure.

The following space filling modes were discovered in the analysed bauxites:

- assembly agglomeration type
- evenly microporous
- evenly compact
- webbed
- collomorph sponge-like
- sceleton type
- leached type

Agglomeration assembly space filling was experienced only in karstic bauxites, whereas collomorph sponge-like and sceleton type space filling was experienced only in laterite bauxites. The remaining types can be found in both of the main types of deposits.

In case of karstic bauxites, the size of the individual mineral grains increases, owing to the loaded strata, but mainly to the tectonic pressure. The loose aggregate space filling, at the same time, starts to be compressed and is transformed into evenly microporous, evenly compressed and finally into textured with large crystals. The period of time - i.e. the geological time - plays a subordinate role, because under undusturbed superposition conditions the aggregate space filling form remained, even in bauxites of the carbonic period.

In bauxites emerged to the surface later the hypergenetic processes bring about secondary-leached type space filling.

Out of the laterite bauxites in the majority of the high situated ones a crystalline, textured space filling has been developed in most of them due to the very strong recrystallization. The primary-leached micro-passages are also frequent. In some deposits evenly microporous and collomorph sponge-like space filling may show up. In samples originating from low terrain situations, evenly microporous and sceleton type space fillings were detected. Space filling is generally more compressed in case of the first group. The reason of the difference is principally explained by the fact that the high situated deposits are laying considerably above the surface level, whereas those of low terrain situation can be found in subsoil water level or hardly above. When the subsoil water level rose - in the rainy season - the bauxite was rearranged and compressed.

Consequently, on the scanning microscope photos of bauxites, principally the deposition mode and the effect of the subsequent processes are indicated. The differences in the mineral composition affect the mode of space filling only to a small extent.

Among the rock-constituent minerals of bauxites the gibbsite and diaspore crystals may grow to the greatest size, whereas the boehmite crystals can only reach a size of a few /um. Hematite and goethite crystals around are a few tenth' /um in size. In bauxites built up of fine grains, greater mineral grains of special shape can generally be found in the micropores.

According to the technological experiences bauxites of small grain-size, irregular grain shape and loose space fill-

ing are digested better and faster than those having the same mineral composition, but of more compressed space filling and more regular crystals.

HARDNESS OF BAUXITE

The hardness of bauxites is a significant parameter as regards their processing possibility: in the knowledge of this parameter the preliminary selection of the bauxite grinding technology /grinding: in ball mill, rod mill, granulitization mill, in open or closed circuit/, and the estimation of the expected wearing-off effects during the process becomes possible.

When defining the concept of hardness, the hardness of the minerals has to be taken as basis, and this concept has to be extended for that of the rock hardness and, specifically, of the bauxite hardness.

In the mineralogy, the concept of the surface hardness of the crystal material is used strictly, meaning the degree of surface resistance of the crystal body against mechanical /principally scratching and abrasive/ effects /141/.

The value of surface hardness depends on which crystal plane /hkl/ it is measured, and it also depends on the direction of the analysis, that is, it is a vector-type value /141/.

The precise hardness testing methods - taking into consideration the orientation - define absolute hardness, and they provide the so-called hardness curves for each individual crystal plane /141/.

The simple methods of hardness determination can only be used for the determination of hardness in perpendicular direc-

tion to the crystals face. Among the latter tests the Mohs hardness determination is the most simple one, providing the relative hardness by comparison with minerals forming a standard hardness-series /141/.

The bauxite as a rock can not be characterized by the above concept of hardness, therefore, this concept will be extended according to practical points of view, and the hardness of the bauxite will mean its resistance against external mechanical effects influencing its form.

Bauxite - being a sedimentary mineral - is the aggregate of fine or relatively fine cohesive grains. The force required to tear out a small grain or an assembly of grains off the basic material /its surroundings/ will not be the function of the individual grain hardness, but of their binding to each other, that is, their cohesion. The hardness of the minerals, though it affects the hardness of bauxite, is of secondary importance.

Aiming at determining the characteristic /average/ rock hardness, several grains have to be involved into the range of tests because of the very different hardness and varying intensity of their adhesion to each other, so a relatively big sized sample must be analyzed. The necessary force to bring about "unit shape deformation" in case of rocks is the function of the size of the analysing equipment, too. Similarly, the plasticity of the rock also affects considerably the degree of resistance, consequently, the velocity of the action of the shape deforming force /velocity of strain increase/ and the rate of the generated deformation also affects the degree of the resistance. The tension distribution /degree and ratio of tensile-, compressive- and shear strains/ of the material induced by the force actions of the applied testing means /graver, pressure plate, etc./ also reacts on the resistivity. The compactness /continuity/ of the material is

also significant. The increase of porosity, for example, progressively decreases the resistance. /Pores and micro-cracks are strain concentration centres, from where the breakage starts./ Reducing the size of the test piece brings about a decrease in the number of location of faults, and thus the solidity increases seemingly, indicating that test pieces of several sizes should be analysed. In case of test pieces of greater size it is a characteristic feature that, besides the orientation characteristic for the minerals, too, the changes of the microstructure /lamellar structure, crack-net, etc./ taking place due to the effects of microtectonic movements at the genesis of the deposit, cause the solidity to be of even more oriented character /81, 82, 83, 138, 139, 140, 114, 142/.

Consequently, samples of several sizes and orientations should undergo standard crushing tests in the laboratory /139, 140/. The series test would create the opportunity to follow-up the intensity of cohesion, in the function of different parameters. The cohesion can be calculated on the basis of the following relationship:

$$c = \hat{\tau} - \bar{\sigma} \operatorname{tg} \Phi \quad ,$$

where: $\hat{\tau}$ = shear stress, in the function of the effective
$\bar{\sigma}$ normal stress,
Φ = internal angle of friction and the slope angle of the tangent of the Mohs stress circles.

The theoretical testing possibility would be to take a sample of correct orientation from the deposit and to produce of it test pieces of regular shape of different sizes and orientation, and to perform compression and shear tests with those at different stress rates. This would be a considerably

time-consuming and difficult test series. Finally, based on the analysis of the results, the relationship with the different measuring units /grindability, wearing-off effect, fragibility, hardness, stoping- and drilling characteristics, volatility, etc./ could also be determined by different technical measuring units, with the knowledge about the functions of the cohesion /c/ changes /139, 140/.

In the practice, however, it is not expedient to perform this test, since the result of a circuitous and tiresome series of tests owing to the great regional inhomogeneity of the bauxite deposits, will be valid for a very little area only. Consequently, measuring units which can directly be used and which are easy to determine are applied, as follows: Mohs-hardness, comminution-, drilling-, stoping- and grinding characteristics. /Drilling and stoping tests of mining character are not going to be discussed herewith, 81, 114, 141, 142, 143, 144, 145, 146, 151, 152, 153./

The Mohs-hardness determination of bauxite is performed by geologists, in the period of geological research. The measured figures provide informatory data for the preliminary design and for the research. On the basis of the Mohs-hardness, the bauxites are classified into 7 hardness groups, and the hardness distribution of the world's stock discovered up to the present has been worked out, too /Table 5.8/.

Grinding hardness test is a suitable figure for evaluating the degree of wearing-off effect, in case it is carried out by grinding a standard material with a determined sized grist /powder/ of the bauxite to be determined, and the wearing-off is measured. The measuring can be connected, for instance, to the determination of the grindability measuring figures, so that the weight reduction of the mill's ball-load is measured /141, 150, 151, 153/.

Comminution test has become the most important indirect measurement of the bauxite's hardness and solidity, respectively, it is easy to perform it in the practice, and it serves as basis during the designing period, for the design of grinding-section and for taking into consideration of the wearing-off effect /144, 145, 146, 151, 152, 153/.

The comminution test can be regarded as the crushing of several test pieces of different shapes and sizes with a different direction of stress. Evaluation is carried out by the special methods of comminution technique. Theoretically, the actual hardness /cohesion/ can also be deduced from the measured figures of special comminution characteristics, but as it does not provide more information for the practice, in most cases it is negligible.

Classification and Distribution of Bauxites According to Hardness

/Gy. Bárdossy: Karstic Bauxites/

Table 5.8

Hardness category	Mohs-hardness	Proportion related to the total reserves, %
1. Extreme hard	above 8.0	1
2. Very hard	4.0-8.0	23
3. Hard	3.0-4.0	22
4. Medium hard	2.0-3.0	15
5. Low hardness	1.0-2.0	20
6. Loose	0.5-1.0	18
7. Unbound	0.1-0.5	1
Total:		100

The validity-range of the grindability measuring units is very limited, being valid only for that medium and type of mill in which it was determined. Consequently, the grindability tests have, by all means, to be performed in the same medium as the grinding in the plant /e.g.: in the digestion liquor/. Water and the surface-active substances /dispersing agents/ dissolved in it reduce the surface tension and the cohesion and this brings about a significant decreasing effect on the grinding energy requirement. Beyond the applied grinding medium, the mode and rate of usage is also affected by the individual mill types. Apart from this, the stress distribution /ratio of compression and shear stress/ depends on other factors, besides the geometrial conditions. On the basis of the above, the production of a model-equipment for grinding technique tests purposes is not a simple task. The theoretical basis of grinding technique tests lies in the fact that efficient energy used for comminution /W_m/ can be determined; moreover, the grain-size distribution of the grist provides the opportunity to test the effect of this energy input, too /81, 138, 142-153/.

The energy consumed for comminution /W_m/, from technical aspects, can be calculated by extracting the /W_k/ energy used for overcoming the external mechanical friction and the energy /W_b/ used up for overcoming the internal friction depending on the mode of operation of the mill from the total energy /W/ required for the operation of the mill /e.g. ball friction and load lifting energy requirements/. The /$W_b + W_k$/ value can be measured in idle-running. The relationship can be described in the $W = W_m + W_b + W_k$ form /81, 83/.

Part of the energy used for the grinding /W_r/ causes flexible deformations and is transformed into heat, thus the actual energy used up for the crushing /W_h/ represents a minor part of the comminution-energy requirement. The relationship can be illustrated in the $W_m = W_h + W_r$ form /81, 83/.

With the help of the above partial energies, two relationships can be produced for the grinding efficiency, of which

$$\eta = \frac{W_h}{W} = \frac{W_h}{W_m + W_b + W_k}$$

is a characteristic relationship both for the equipment and the material, whereas the following relationship,

$$\eta = \frac{W_h}{W_m},$$

gives a characteristic efficiency principally for the material /its flexibility, plasticity/ $/\eta_t \ll \eta_m/$.

Approaching the problem from the point of view of the ground material, the value of the efficient energy $/W_m/$ can be deduced /though only approximately/, on the basis of the so-called "grinding theories". According to the first /Rittinger /153/ comminution theory, the comminution energy requirement is proportional to the originated new surface, whereas the second theory /Kirpicsev /149/ and Kick /150/ / states that it is proportional to the original volume /size/ of the grains.

Bond combined the two rules into a so-called third rule /151, 152/ which is theoretically more reliable. Later the theory was further developed, as not only a certain notable grain-size was taken into consideration but the grain-size distribution itself, too /1, 12, 13, 20/. The most general formula can be described as follows:

$$W_m = C_i \left(\frac{1}{n_2 \cdot x_2^{k_2}} - \frac{1}{n_1 \cdot x_1^{k_1}} \right) \quad \left(J/m^3 / \right)$$

where: x_1 = 80 per cent amount of the original distribution
x_2 = 80 per cent amount of the fracture distribution
C_i = the so-called "energy index"
n_2 = regularity factor of the original RR* distribution function
n_1 = regularity factor of the RR fracture distribution function
k_1 and k_2 = exponents

*Note: RR is the symbol of the Rosin-Rammler grain-size distribution function.

If $k_1 = k_2 = 1/2$ and $n_1 = n_2 = 1$, the original Bond formula is obtained, but it can be that $k_1 = n_1$ and $k_2 = n_2$, too. /The Schumann distribution function can not be used!/ /81/

The C_i energy index is generally given as the energy requirement for grinding a material of the same mass /J/g/ or of the same volume /J/cm^3/ /81, 145, 153/.

A generally applicable method is provided on the basis of the above principles for the comparison of the grindability of certain materials /in the same mill/ or for the selection of the most efficient mill type related to a certain material and to optimize its operational parameters /81, 145, 146, 153/.

Bond elaborated his standardized grinding technique test after the optimization of the operational conditions of the

ball mill. The essence of the test is that the specific energy requirements of different materials /c_3/ can be determined by their dry or wet grinding in a standardized ball mill with similar grinding energy input /during 100 turns of the mill/ /81, 83, 145, 146, 151, 152/.

The result can also be given by calculating the grinding energy requirement of the materials from their infinite grain-size /$x_1 = \infty$, surface energy content = 0, because $1/\sqrt{x_1} = 0$/ to below 100 /um /the surface energy increment being x_2 = = 100 /um/: i.e. W_i, the so-called "comminution index" on the basis of the following formula /81/ is:

$$W_i = c_3 \frac{1}{\sqrt{100}}$$

This W_i index can be used further similarly to constant c_3 of the specific energy requirement /81/. The energy requirement of an optional degree comminution is namely:

$$W = W_i \frac{\sqrt{x_1} - \sqrt{x_2}}{x} \cdot \sqrt{\frac{100}{x_2}} = W_i \frac{\sqrt{\nu} - 1}{\sqrt{\nu}} \cdot \sqrt{\frac{100}{x_2}} \quad /J/cm^3/$$

where: $\nu = x_1/x_2$ = degree of comminution

The facts detailed up to now refer to the single grinding, that is the so-called "open grinding", whereas the Bond test can be used for constructing a model of the circuit grinding process as well. Stopping the mill after 100 turns, the grist is screened through a sieve corresponding to the required grinding fineness /320 /um, for example/, the material fallen through the sieve is weighed and the coarse fraction is sup-

plemented by the raw material of the same amount, to bring it up to the original amount. The process is repeated as long as the amount of the material falling through the sieve becomes constant. The amount of originally finer grains is subtracted from the stationary amount, then the remaining weight is divided by the number of revolutions: the resulting /G/g/rev./ weight is called the "ball mill grindability". The sieve residue determines the recycling coefficient. The recycling coefficient is generally accepted in advance to be 250 per cent, but in this case the revolution number of the second and the subsequent stages must also be calculated /and it will not be 100/. Of the 3.5 g material fed in per one revolution, 1 g final product is to be gained during the same period which is called "intentional final product". On the basis of the latter, the empirical work-index reads:

$$W_i = \frac{16}{0.82} \cdot \sqrt{\frac{x_H}{100}}$$

where: x_H = represents the size of the opening of the limit screen.

/In case if for the recycling coefficient a different value is given than 250 per cent, the above formula is no longer valid, and the whole calculation method of the c_3 index has to be carried out; 81, 146, 151, 152, 153./

It has to be mentioned that the Bond test is applicable even in case if only the lognormal distribution can be used instead of the RR distribution, though in this case the calculation is much more difficult. The Bond energy theory includes any other theories as limitations or intermediate cases, consequently, its application is unlimited /81/.

The Hardgrove number is the other grindability measuring unit /146, 147/. It is rather easy to determine, but it has a disadvantage, namely, that it is suitable to the dry tests only. Its mechanical and technical value is low, as regards the alumina industry. It can only be used for testing the grindability of any ore, in case the validity of the Rittinger /surface/ theory is provable, but this applies only in case of coarser grinding /81, 146/.

It has become widespread in practice very quickly due to its simplicity. /This can not be stated about the Bond test./

The means of determination is the so-called Hardgrove mill, a ring-shaped grinding vessel in which 8 balls of 25.4 mm diameter are rolling with constant load. From the sizes falling between 0.59 and 1.19 mm, and produced from the sample by screening, 50 g grain fraction is measured in for a test. The result can be calculated by means of the following relationship:

$$H = 13 + 6.93\ W$$

where: W = the amount of the material /g/ fallen through the 0.074 /um mesh screen.

DENSITY OF BAUXITES

In the course of a complex investigation of bauxites aiming at determining their commercial value and processibility the density respectively volumetric density are also determined.

The knowledge of density respectively volumetric density of the bauxite will be of importance at the areas and functions as follows:

- mining: - account of production
  - checking of the ore kept in the stockyard
- alumina plant design:
  - dimensioning of the transporting systems, stockyards and equipment
  - calculation of the technological material balance
- alumina production:
  - control and inspection of the process in the alumina plant

The density of bauxites is the mass comprised in the unit volume.
Its dimension is: g/cm^3 or kg/m^3.

Considering that the bauxite is a heterogeneous material the density of bauxites is the average density of minerals constituting the bauxite, its value being the function of the mineral composition of the bauxite.

Average density of main componenets of the bauxite are enumerated in Table 5.9, while the density of some bauxites are shown in Table 5.10.

Density of Main Mineral Components of the Bauxite

Table 5.9

Mineral	Density, g/cm^3
Gibbsite	2.39
Boehmite	3.04
Diaspore	3.40
Goethite	4.30
Hematite	5.25
Anatase	3.90
Rutile	4.20
Kaolinite	2.65
Quartz	2.66
Calcite	2.68
Dolomite	2.85

Density of Bauxite and Red Mud Samples at 25 °C

Table 5.10

Place of origin		Density, g/cm^3	
		bauxite	red mud
Ghana:	Kibi	2.73	3.05
	Aya Nyinahin	2.75	3.05
Greece:	Eleuses	2.95	-
India:	Amarkantak	2.86	3.20
Jamaica:	S.Manchester	2.70	2.97
Jugoslavia:	Vlasenica	2.85	-
	Niksic	3.19	-
	Kosovo	3.01	-
Hungary:	Halimba	2.87	3.20
	Iszkaszentgyörgy	2.91	3.18
Vietnam:	Lang Son	3.00	-

The change in the bauxite composition, the effect of some minerals on the density of bauxite are shown below:

Type of bauxite	Density, g/cm^3
Gibbsitic, goethitic /hematitic/ /Jamaica/	2.7-2.8
Gibbsitic-boehmitic, hematitic-goethitic /Hungary/	2.8-3.0
Diasporic-hematitic /Greece/	2.9-3.2

It can be seen from the above that the density increase as the gibbsitic feature of bauxites decreases /even a nearly similar Fe_2O_3 content/.

Several methods may be used for the determination of density of bauxite, however, the well known pycnometer method is the most widely used and the most expedient one, as it is easy to perform.

VOLUME DENSITY OF BAUXITES

By the volume density /apparent density/ of bauxite the mass of lumpy bauxite which can be filled into the unit volume /usually 1 m^3 or litre/ is meant. Its dimension is: kg/m^3 or g/l.

When determining the volumetric density the tested lumpy bauxite is filled under identical circumstances into a container having unit volume and the mass of the filled in bauxite is weighed.

The volumetric density is influenced by several factors /the grain-size of the bauxite, its moisture content, degree of standardization of the measuring conditions, etc./, thus

the comparison of these figures is only possible if the results were obtained by following strictly similar methods.

PHYSICO-CHEMICAL INVESTIGATION OF RED MUDS

SPECIFIC SURFACE AREA OF RED MUDS

The specific surface area of red muds depends on the quality of bauxite, the amount of the individual components, and the processing technology. The extent of the surface area of red muds produced at identical parameters of a given technology influences its settling and filtration capability. In order to illustrate the above the filtration capacity is plotted vs. the specific surface area in Fig. 5.6. As it can be established from the relationship the filtration capacity decreases if the surface increases. This /in addition to the relationship between the grain-size and pore size/ is the consequence of the fact that the red mud having larger specific surface area and higher /surface/ energy related to the unit weight agglomerated better, the energy of interaction among the particles is higher, thus the filter cake becomes compacter and the filtration capacity decreases.

POROSITY AND PORE SIZE DISTRIBUTION OF RED MUDS

The pore size distribution of red muds preserves the character of the pore size distribution of the corresponding bauxites /Fig. 5.7/. The knowledge of their porosity and pore size distribution can be utilized in the determination of the morphology of the red mud and in the industrial scale in the red mud washing process. An actual example can be given for this in the Pikalevo alumina plant /Soviet Union/ where the porosity of the burnt nepheline ore is routinewise measured in the plant and the parameters of leaching respectively washing are set accordingly /73/.

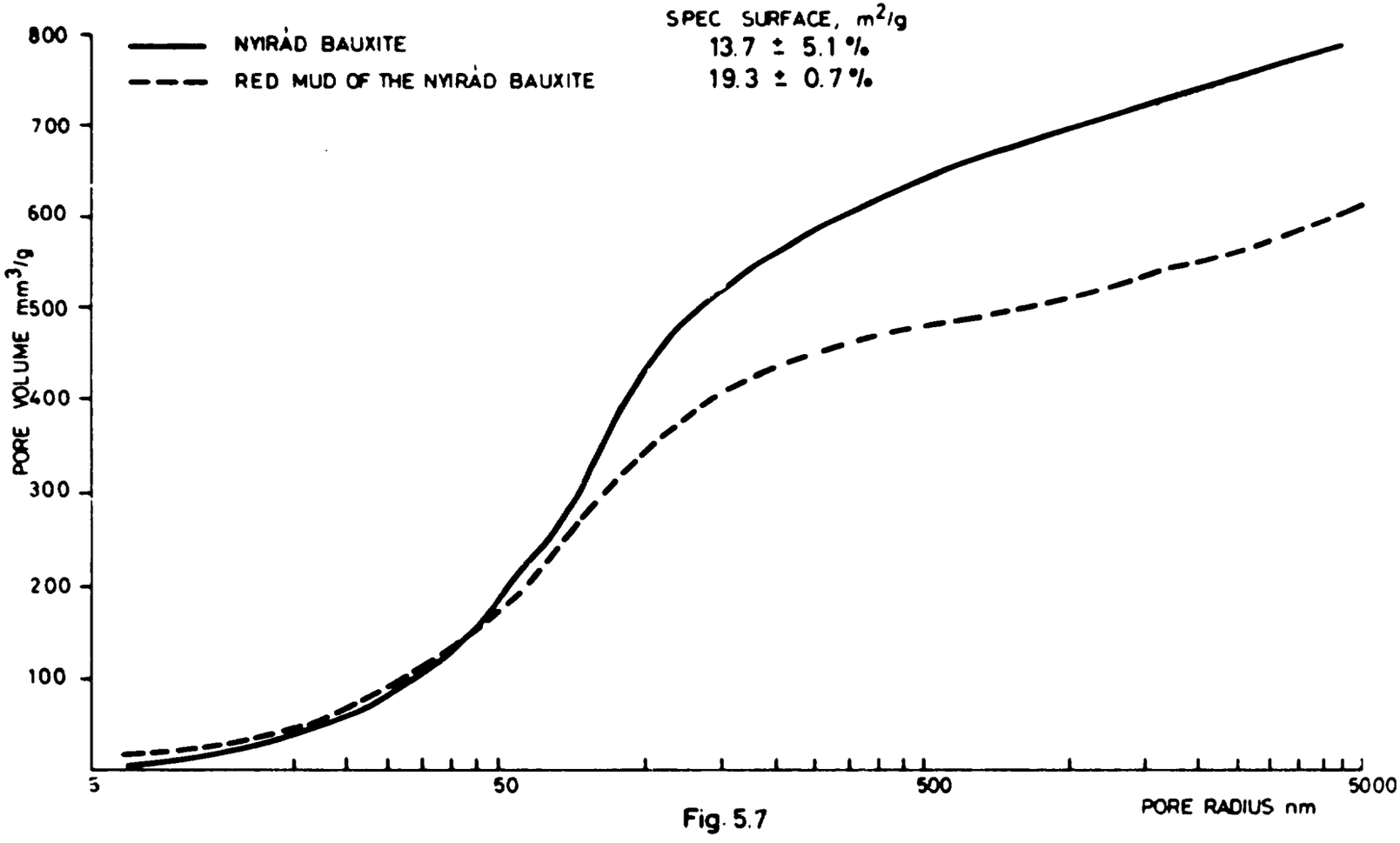

Fig. 5.7

PORE SIZE DISTRIBUTION OF BAUXITE AND OF ITS RED MUD

IMMERSION HEAT OF RED MUDS

Tables 5.7 and 5.11 provide information about the immersion heat values measured with red muds and red mud components in water. On basis of the data it has been established that the above materials are powders possessing high surface energy. The immersion heat values lie mostly in the range of 0.16-1 J/m^2. The data of the tables furnished information for the optimization of the operation of the Dorr-type settlers in the alumina plant. The immersion /adsorption/ heat relations determined on the same red mud in the functior of concentration or molar ratio of the sodium aluminate liquor can also be used for the same purpose. The relationship given in Fig. 5.8 draws attention to the dependence of the adsorption of the organic substance on the molar ratio and also enables the determination of the molar ratios corresponding to the maximum respectively minimum adsorption.

Immersion Heat of the Red Mud Components

Table 5.11

Material	Immersion heat, $Joule/m^2$
$Mg_4Al_2/Al_2SiO_2/O_{10}/OH/_8$ *	0.660
$3CaO.Al_2O_3.kSiO_2/6-2K/H_2O$ *	0.848
$3NaAlSiO_4 \cdot Na_2CO_3$	1.450
$MgAl_2O_4$ *	0.745
$CaTiO_3$	0.697
FeO/OH/	0.386
$MgTiO_3$ *	1.684

*The asterisked materials resulted during Bayer digestion in the reaction of dolomitic bauxite with the aluminate liquor.

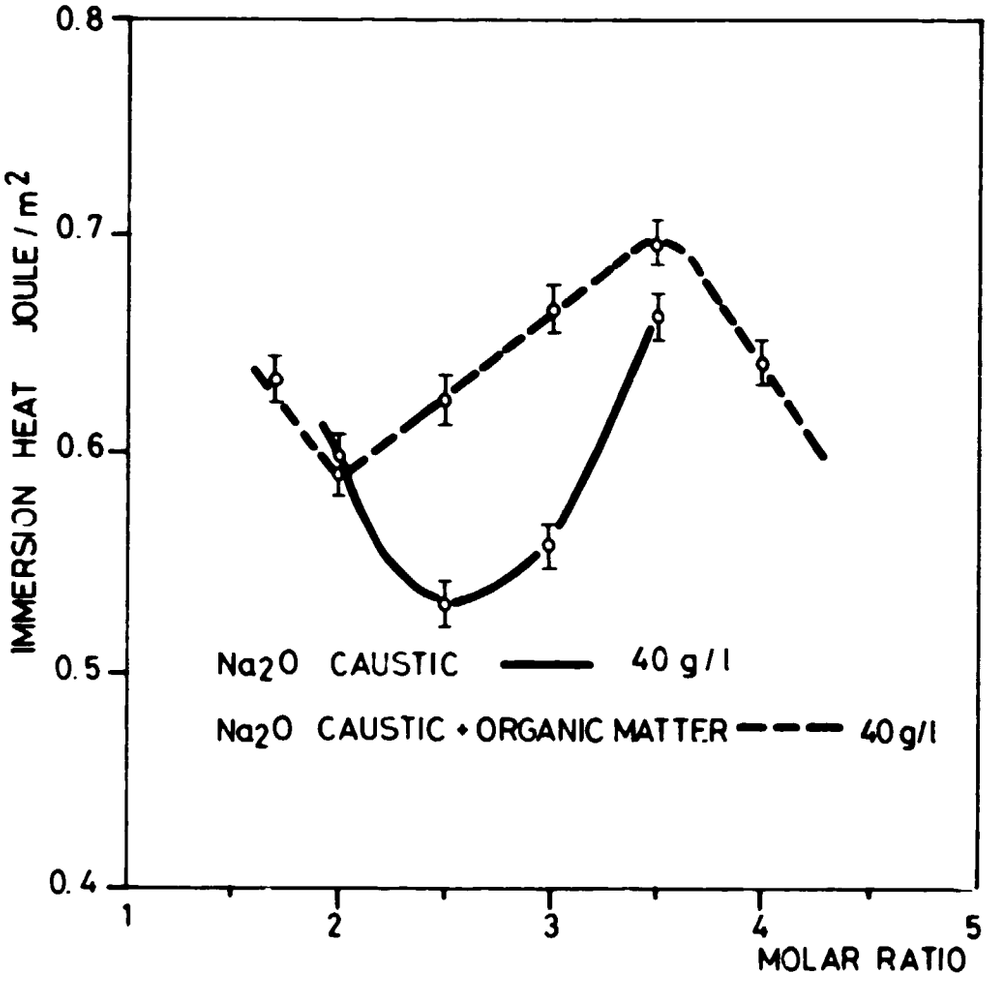

Fig. 5.8

CHANGE OF THE IMMERSION (ADSORPTION) HEAT OF THE RED MUD IN THE FUNCTION OF THE MOLAR RATIO OF THE SODIUM ALUMINATE LIQUOR

MORPHOLOGY OF RED MUS

GRAIN-SIZE DISTRIBUTION OF RED MUDS

The phase conditions of the Al_2O_3-Fe_2O_3-H_2O system /133/ and the Fe_2O_3-H_2O system /134/ and their possible phases those have been examined by Wefers during his systematic investigation he has studied the morphology of the individual phases by means of a transmission electron microscope. From the point of view of the modification of the technological processes not only the morphological properties of the raw materials, however, those of the intermediate products, i.e. the components of the red mud are of importance /135, 136/. The morphological properties are of importance from the point of view of the technological processes, the separation of red mud and the washing possibilities. The amount of the solution retained in the material depends on the total volume of pores while the washability of it depends on the size of the pores.

The small grain-size product formed as the result of the chemical process is in majority in the red mud. These particles, mainly less than 100 nm in size, surround and cover the larger ones, for instance the undigested mineral particles. Just due to their small size and owing to their heterogeneous state the transmission electron microscope is primarily suitable for their testing. The following statements have been made /137/ in the course of testing red muds and its individual components by means of the direct transmission electron microscope respectively covering replicae, and by means of the scanning electron microscope:

In the red mud /specific surface area 18.4 $m^2/g \pm 1.6$ %/ every kind of individual particle sizes ranging from few-fold 10 nm to several times 10,000 nm can be observed. Size of majority of the particles is about 100 nm. They are mainly cigar shaped /goethite/ and their minor portion has a hexagonal facet from /hematite/.

The synthetically produced chloride sodalite /specific surface area 12.2 $m^2/g \pm 2.2$ %/ is composed of individual crystals of different size ranging from 100 nm to several times 10,000 nm. These are angular facelets resp. small plates definitely liable to agglomeration.

The synthetically produced goethite /specific surface area 115.4 $m^2 \pm 1.9$ %/ is composed of needle respectively cigar shaped particles 10-100 nm in size. These particles aggregate in a material-like form.

The synthetic Ca-aluminate /specific surface area 1.3 m^2 $\pm$ 5.7 %/ consists of mainly rounded-off particles ranging from 100 nm to 10,000 nm in size. The rounded-off shape enables only loose coherence. Within the $\sim$ 10 /um /10,000 nm/ particles the crystalline particles smaller by about 2 orders of magnitude are located. The synthetic Mg-AlSi /specific surface area 37.7 $m^2 \pm 0.4$ %/ consists of comparatively uniform small plates about 100 nm in size. Due to the above mentioned shape and size it can easily agglomerate to larger aggregations.

The above outlined morphologic features motivate the different effects of various phases constituting the red mud on its settling and washability, and the formation of the pore structure, i.e. the void places of the lattice structure composed of the particles described above.

DENSITY OF RED MUDS

The definition and the determination of the density of red mud is analogous to that described in case of bauxite. Its value ranges from 3.0 to 3.5 g/cm^3 depending on the mineral composition of the mud.

The increase of hematite content of red mud and/or the decrease of the amount of undigested Al-minerals result in the increase of density.

The knowledge of the density of red mud is very important at the mechanical and structural designing of the equipment, furthermore at the plant control and supervision /for instance red mud settling and washing/ in the alumina plant. The density values of some red muds are enumerated in Table 5.10.

PHYSICO-CHEMICAL INVESTIGATION OF ALUMINA HYDRATE AND ALUMINA

SPECIFIC SURFACE AREA OF THE ALUMINA HYDRATE AND ALUMINA

The specific surface area of the alumina hydrate depends on the technology and the parameters of the precipitation process. The knowledge of the extent of the surface area of the alumina hydrate supplies useful information for the improvement of the efficiency of precipitation. In certain plants, particularly in those producing sandy alumina - the amount of seed hydrate to be charged to the precipitation process is determined by the help of the measurement of its specific surface area.

The specific surface area of the coarse-grained or so-called sandy alumina hydrate exceeds several times that of the floury alumina produced by the European Bayer technology. While the latter has a specific surface area of 0.1-0.2 m^2/g the former can even attain at 0.6 m^2/g. By a special process a bayerite-type $Al/OH/_3$ having a specific surface area of 200-300 m^2/g can also be produced.

The calcination process of the alumina hydrate can be fairly traced by the measurement of the specific surface area /Fig. 5.9/. In order to illustrate the above the change of the spe-

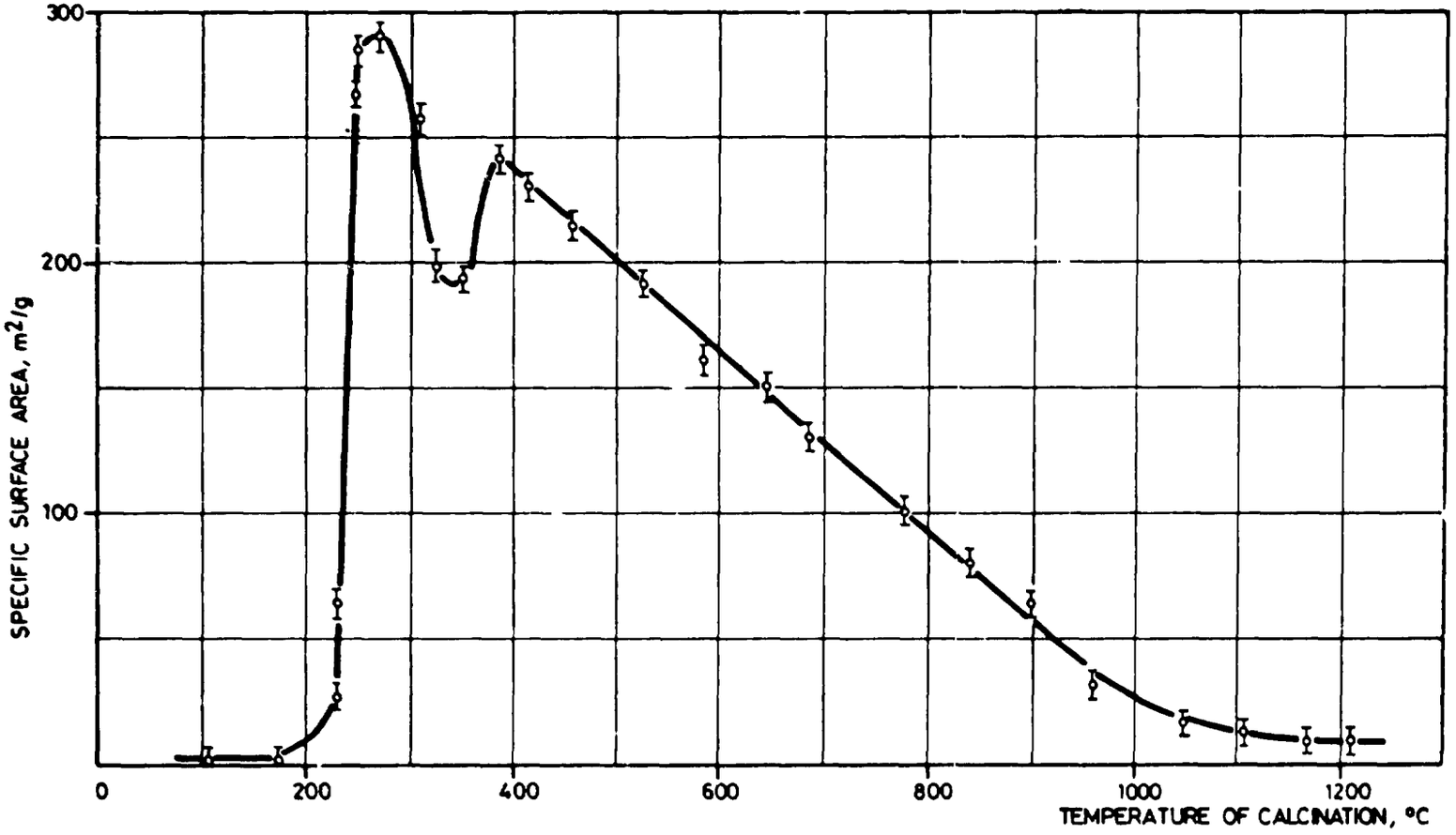

Fig. 5.9

THE CHANGE OF SPECIFIC SURFACE AREA OF THE ALUMINA HYDRATE AND ALUMINA, RESPECTIVELY, IN THE FUNCTION OF THE TEMPERATURE OF CALCINATION

cific surface area of the $Al/OH/_3$ and the Al_2O_3 has been plotted vs. calcination temperature in the figure. The curve fairly indicates the temperatures of the water-release of the $Al/OH/_3$ and decrease of specific surface area connected with the transformation of the crystal structure of the Al_2O_3.

On basis of the figure it can be established that the specific surface area of the "properly" calcined /having higher α-alumina content/ alumina is in the range of 5 to 20 m^2. /This figure is in good agreement with those measured in the plant./

The above values relate to the alumina produced by the European Bayer technology. The surface area of the alumina produced by the American Bayer technology, is in the range of 30-100 m^2/g. /Table 5.12/

Physico-Chemical Properties of Alumina Samples

Table 5.12

Grain-size distribution /%/	ALCAN-Ewarton plant	ALCAN-Kirkwine plant	ALCOA	ALPART	Stade	Ajka-2
above 160 ,u	0	0	5.8	7.8	0.1	0
100-160 ,u	38.4	5.4	34.9	39.2	9.9	8.6
80 -100 ,u	34.0	23.8	25.2	24.6	15.0	8.4
71 - 80 ,u	12.0	21.4	10.2	6.2	11.0	2.8
63 - 71 ,u	4.0	2.8	5.0	4.2	5.4	15.0
56 - 63 ,u	5.4	16.2	5.1	5.4	10.2	2.2
45 - 56 ,u	5.0	18.6	6.6	6.0	22.0	18.0
below 45 ,u	1.2	11.8	7.2	6.6	26.4	45.0
30 - 45 ,u	0.5	2.4	0.6	0.9	2.4	5.9
20 - 30 ,u	0.6	8.3	3.4	3.3	11.3	13.0
10 - 20 ,u	0.1	1.0	2.5	1.9	9.7	12.3
0 - 10 ,u		0.1	1.0	0.5	3.0	13.8
Average grain-size Ø ,u	81.1	61.2	85.6	89.6	53.4	39.4
Characteristics of the material	1	2	3	4	5	6
α-content, %	4.0	17.0	36.0	11.0	5.6	55.8
angle of repose, ^{o}	31.80	32.95	35.45	33.75	-	34.8
specific gravity	3.23	3.46	3.69	3.43	3.51	3.80
loose volumetric density, g	967	926	966	927	-	1011
shaken volumetric density, g	1120	1120	1170	1110	-	1340
specific surface area, m^2/g	102.1 ± 3.8	74.8 ± 1.2	31.5 ± 3.4	66.2 ± 1.6	56.2 ± 1.6	6.2 ± 2.5

POROSITY AND PORE VOLUME DISTRIBUTION OF THE ALUMINA HYDRATE AND ALUMINA

The $Al(OH)_3$ crystals consist of very poor porosity particles limited by comparatively compact crystals /22/. The very small specific surface area values are also indicative of the former statement. The knowledge od their porosity and thus the pore size distribution has no practical importance.

According to their comparatively large specific surface area the aluminas are highly porous substances. It is particularly important to know the porosity and pore size distribution of the special Al_2O_3-base products /adsorbents, siccatives, catalyst carriers, fillers and abrasives/ the surface area of which exceeds 100 m^2/g /Fig. 5.2/. It can namely be established from the data of the size distribution to what extent the pores of the adsorbent are accessible for the adsorbate.

In the case of catalyst carriers the possibility to carry the catalyst layer onto the carrier, and the possibility of the penetration of the substances to be catalyzed into the pores can be decided with the knowledge of the distribution.

In the case of fillers the bond strength between the filler and the basic substance may depend on the pore size. In this case, the requirement in relation to the filler is a stipulated and optimal pore size, and pore size distribution, respectively.

In case of abrasives the pore size distribution curve gives information about the strength of the particles and the amount of grinding edges, corners, etc.

In the case of alumina produced for metallurgical purposes the knowledge of porosity and pore size distribution is of less importance /Fig. 5.4/. Their knowledge can give infor-

mation about the strength of the particles. If the alumina is used for binding the fluorine content of the stack gases of the smelter, in order to meet the requirements of the ecological protection, the knowledge of the distribution function will become necessary on the basis of reasons mentioned at the adsorbents.

IMMERSION HEAT OF THE ALUMINA HYDRATE AND THE ALUMINA

In the case of the alumina hydrate and the alumina the immersion heat has no practical importance. When grading these materials, furthermore when characterizing their behaviour under varying technological conditions, however, it is already widely used. It is felt to be useful for the characterization of the "adsorption capacity", "surface energy level" and - transferred - "activity" of the hydrates of various grain-size. The order of magnitude of the immersion heat of a product hydrate for various times of storing is given in Table 5.13.

The Change of Immersion Heat in the Function of Time

Table 5.13

Denomination	Adsorption/immersion heat Joule/m^2	Storing medium
Product hydrate from Magyaróvár	1.322 ± 5.5 %	Sodium aluminate liquor; of 100 g/l Na_2O caustic concentration and 2.5 molar ratio
Product hydrate from Magyaróvár after storing for 312 hrs	1.162 ± 3.1 %	
Product hydrate from Magyaróvár after storing for 816 hrs	1.063 ± 4.2 %	
Product hydrate from Magyaróvár after storing for 1488 hrs	0.977 ± 2.3 %	
Product hydrate from Magyaróvár after storing for 2736 hrs	0.744 ± 5.4 %	
Product hydrate from Magyaróvár	1.322 ± 5.5 %	3 % HCl solution
Product hydrate from Magyaróvár after storing for 312 hrs	1.042 ± 3.2 %	
Product hydrate from Magyaróvár after storing for 816 hrs	0.898 ± 3.3 %	
Product hydrate from Magyaróvár after storing for 1488 hrs	0.907 ± 5.1 %	
Product hydrate from Magyaróvár after storing for 2736 hrs	0.663 ± 8.6 %	

MORPHOLOGY OF THE ALUMINA HYDRATE AND ALUMINA

GRAIN-SIZE DISTRIBUTION OF THE ALUMINA HYDRATE AND ALUMINA

The aluminium hydroxide crystals produced during the precipitation process in the Bayer process are always mainly of the polycrystalline character. The informations concerning the polycrystalline character of the aluminium hydroxide had been based on investigations carried out by means of the optical and transmission electron microscope up to the 70s /116, 117, 118/. High impulse was given to the research work by the use of the scanning electron microscope /119, 120/.

The aluminium hydroxide monocrystals belong to the monoclinal crystal system and occur in the form of pseudo hexagonal platelets and prisms. The various modifications of the perfect form came into being by polycrystallization. The most important types of the latter are as follows:

- crystals which came into being by normal growth
- crystals bearing needles and platelets on their surface having come into being by abnormal growth
- aggregations and agglomerates of the two former.

It is easy to discriminate aggregations from agglomerates morphologically. This can partly be made on the basis of the shape of the polycrystals partly on basis of the surface morphology. The crystals forming the agglomerates tightly coalesce, no sharp boundaries can be found at the juncture of the crystals and their shape is of symmetrical structure. The aggregations are built up of sharply discriminated crystals and at some places gaps can also be found among them.

According to the literature of this area the largely oval particles come into being by the aggregation of smaller crystals and the spherical particles, in turn, mainly by the growth of the seed crystals present in the solution.

The formation of small-sized / 10,000 nm/ particles is promoted by the following factors:

a/ due to high oversaturation /contamination, amount of seed hydrate/ of the solution numerous secondary crystals can form which, depending on the circumstances of stirring, can break off the surface of the seed crystals;

b/ in case of vigorous stirring several small crystals get into the solution due to fragmentation and wear of the particles.

According to the character of space utilization of the aggregations one can differentiate among loose aggregations being composed of many crystals of different size, more compact aggregations composed of nearly similar sized crystals and aggregations wherein the constituting crystals are tightly grown together /agglomerates/.

The character of the space utilization is in close relationship with the technological conditions, for instance the vigorous stirring hinders the agglomeration and if loose aggregations are dominating in a sample, a vigorous stirring can be supposed.

The dissected surface structure on the individual crystals is traceable to the deficiency of growth.

From the technological point of view the following proved to be the most important morphologic parameters of the aluminium hydrate polycrystals /121/:

- Size and shape of the particle
- Space fillung up of the aggregations
- Surface structure
- Waved basis plane
- Waved prism plane
- Peeled off peaks and edges
- Number and size of the secondary crystals

By particle size in the case of spherical shaped particles the diameter is meant, in the case of oval grains, in turn, their length and width is meant, the quotient of the two is characteristic of the deviation from the spherical shape. The peeled off peaks and edges may be in connection with the intensity of stirring.

The quantitative evaluation of the morphologic content /particle size distribution, connection between size and shape, size of the individual crystals, size of the agglomerates, number and size of the secondary crystals/ of the scanning electron microscope shots is carried out by means of picture analyzers /122, 123/.

The combination of the scanning electron microscope and the picture analyzer has been used by White and collaborators for the characterization of aluminium hydroxides and oxides of different origin /124, 125/.

In the practice, from the point of view of the technology, both the morphology and the grain-size have decisive role. This statement is true in the formulation according to which also the technology decisively affects the morphology, grain-size and distribution of the alumina hydrate. This relation is unequivocally proved by the alumina hydrates resulting in the precipitation processes of both the European and American Bayer technology /121/.

The morphology, grain-size and grain-size distribution of the alumina hydrate is also decisive from the aspect of the corresponding physico-chemical properties of the alumina. This is particularly important, because during the calcination of the alumina hydrate generally peeling-off occurs. This statement is not valid in every case when calcination is carried out in the presence of mineralizators.

The researchers have been highly concerned themselves for some decades with the transformations, recrystallization, water release and morphologic changes taking place under thermal effect of the aluminium hydroxide - oxidehydroxide - oxide system. The starting materials, production methods test conditions and vide variety of testing methods resulted in a large stock of literature /126/.

Materials produced by heat treatment became more and more important from the point of view of practical use. In the course of their application apart from the chemical and physical structure the morphologic properties proved to be also important /127/. The size shape and surface structure of the particles formed by the calcination of aluminium hydrate produced in the course of the Bayer process decisively affect the properties related with material handling and transport: the angle of repose, the volumetric density and the liability to dusting.

The morphologic parameters are directly connected with the chemical and physico-chemical features of the material, for instance with the solubility in cryolite or with the water adsorption.

Concerning this relation some more examples can be found in the application of aluminium oxides for other industrial use, too /adsorbents, catalysts, abrasives, etc./ /128/.

The morphologic conversion of the products resulting during the heat treatment of aluminium hydroxides has been studied by Wefers by means of the transmission electron microscope /129/. He stated that the dehydration of gibbsite took place during the laminar splitting of the original gibbsite crystal. It is known on the basis of other measurements that the conversion process highly depends on the antecedents of the aluminium hydroxide - aluminium oxide. By the help of

transmission electron microscopic tests carried out on products obtained by the heat treatment at 825 °C, 1200 °C and 1400 °C of industrial aluminium hydroxides from Ajka with 40,000 to 60,000 nm dimensions the internal crystalline structure of the transforming pseudohexagonal configurations could be observed /130/. The internal recrystallization of the pseudohexagonal configurations is also accompanied by the change of the surface morphology. This had been studied by the help of covering replicae in transmission and scanning electron microscopes, respectively /131, 132/.

According to observation, the morphologic change of the surface area of the pseudohexagonal particles occurs at the heat-treated state at which, according to the X-ray tests, the formation of the α-Al_2O_3 phase has already started. According to the X-ray tests if a product, containing already 100 % of α-Al_2O_3 is further heat-treated the surface structure will change further. This change of the surface can be explained by the recrystallization process of the stable phase.

On the original gibbsite forms in the course of calcination the coarsening and furrowing of the surface becomes more intensive depending on the temperature and time of heat treatment. This is the morphologic consequence of the forming laminar structure. Additives highly influence the morphologic changes.

Examples of the grain-size and distribution of alumina are shown in Table 5.12. In the rable numeric values of some of their physico-chemical features are also given.

81 01 13

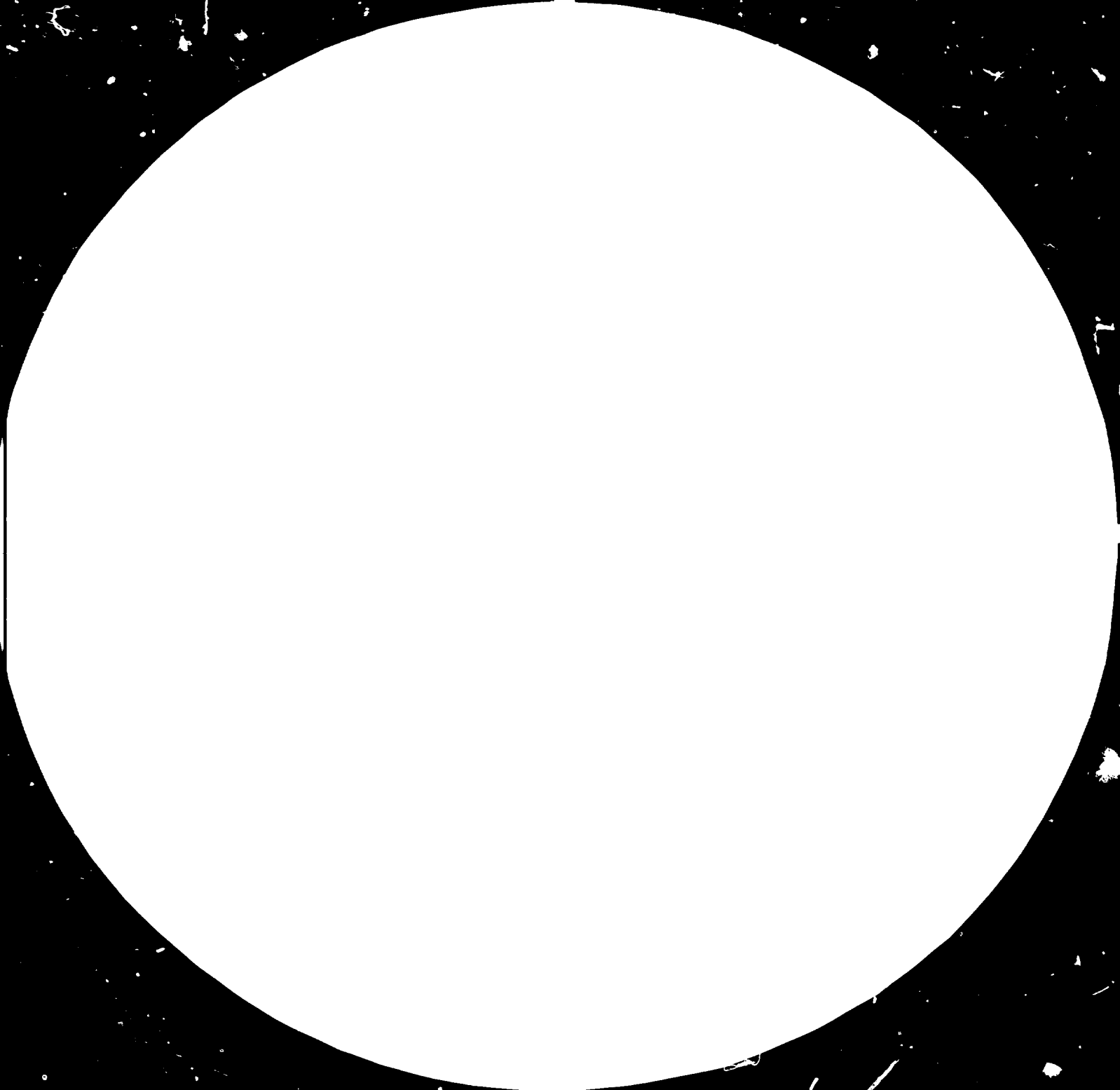

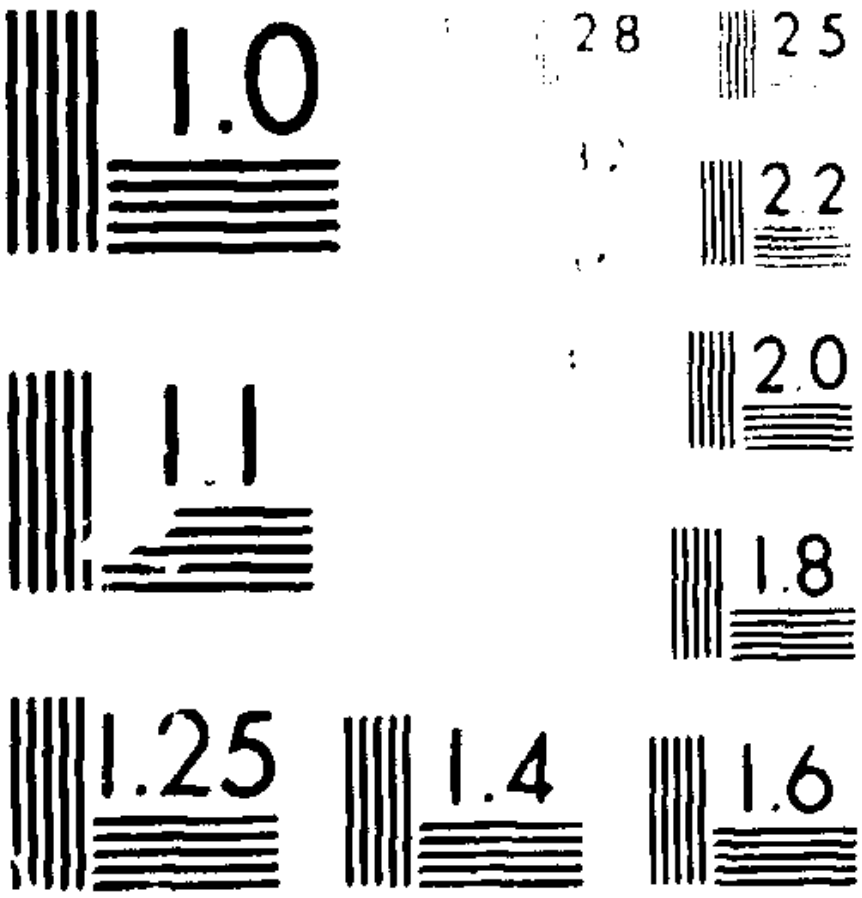
2.8
2.5
1.0
2.2
2.0
1.1
1.8
1.25
1.4
1.6

DENSITY AND APPARENT DENSITY OF THE ALUMINA HYDRATE AND ALUMINA

The definition and determination of the density of the alumina hydrate and alumina is analogous with those described in previous Chapters for bauxite and red mud.

The knowledge of the density will be of importance at the designing work, control and supervision of the production and the metallurgical utilization of the alumina.

The knowledge of the apparent density of the alumina is even more important because this provides indirect information about very important parameters, i.e. the grain composition and the surface condition of the particles, connected with the grading and qualification of the alumina.

The apparent density varies according to the type of the alumina produced /floury or sandy/ in the following ranges:

Type of alumina	Apparent density, g/l
Floury alumina	950-1050
Sandy alumina	850- 950

The density and apparent density of some alumina samples are indicated in Table 5.14.

Density and Apparent Density of Alumina Samples at 25 °C

Table 5.14

Place of origin		Density g/cm^3	Apparent density g/l
Czechoslovakia:	Ziar	-	1017
Jamaica:	Alcan-Ewarton	3.23	967
	Alcan-Kirkwi.ie	3.46	926
	Alcoa	3.69	966
	Alpart	3.43	927
Hungary:	Ajka 2	3.80	1011
	Almásfüzitõ	3.70	1125
W.Germany:	Stade	3.51	-
Italy:	Porto Marghera	-	970
USA:	Baton Rouge	-	930

THERMAL CONDUCTIVITY OF ALUMINA

The thermal conductivities of the various aluminas differ from each other. The thermal conductivity is necessary first of all at the calculation of the heat balance of the aluminium electrolyzing cells.

The fine-grained "floury" or "sticky" aluminas are of heat insulating character, while the coarse-grained "sandy" aluminas are the best heat conductors.

For the measurement of the thermal conductivity the so-called Nusselt double spheres are used.

The thermal conductivity can be calculated as follows:

$$Q = \lambda \frac{F}{r} /T_1 - T_2/ \qquad /1/$$

where: F = the surface area, m^2

r = width of the wall or insulating material, m

T_1 = the higher temperature value, ^oC

T_2 = the lower temperature value, ^oC

λ = thermal conductivity factor /mh^oC

wherefrom the thermal conductivity factor reads:

$$\lambda = \frac{r}{F} \cdot \frac{Q}{T_1 - T_2} \qquad /2/$$

As the material to be tested is positioned between two concentric spheres, r will change between two given values

/r_1 and r_2/, the area F is the function of r, accordingly the previous equation can be written directly only for an infinitesimal dr layer thickness, and the desired value can be obtained by the definite integral of the same:

$$\frac{r}{F} = \int_{r_1}^{r_2} \frac{dr}{4r^2\pi} = -\frac{1}{4\pi}\left[\frac{1}{r}\right]_{r_1}^{r_2} = \frac{1}{4\pi}\,\frac{r_2 - r_1}{r_2 \cdot r_1}$$

If instead of tne radii the diameter is used for the calculation and Q = 0.86 . V . I is substituted irto the equation, we shall obtain:

$$\frac{r}{F} = \frac{1}{2\pi}\,\frac{d_2 - d_1}{d_2 \cdot d_1} \qquad /3/$$

then we come to the relationship:

$$\lambda = \frac{1}{\pi} \cdot \frac{0.86 \cdot V \cdot I\ /d_2 - d_1/}{/T_1 - T_2/\ d_2 \cdot d_1} \qquad /4/$$

where: λ = thermal conductivity factor, kcal/mh^{o}C

V = voltage of the electric range, V

I = current intensity over the electric range, A

T_1 = average temperature of the outer surface of the internal sphere, ^{o}C

T_2 = average temperature of the internal surface of the external sphere, ^{o}C

d_1 = diameter of the internal sphere, m

d_2 = diameter of the external sphere, m

The thermal conductivity factor is established as the value pertaining to the average temperature of

$$\bar{T} = \frac{T_1 + T_2}{2}$$

The thermal conductivity factor is a function of the temperature. At the temperature level /110-130 ^{o}C/ of the alumina layer covering the surface of the aluminium electrolyzing cells the thermal conductivity factor varies depending on the type of alumina in the range of 1.3 to 1.6 kcal/hm^{o}C.

FLUORINE ADSORPTION OF THE ALUMINA

In the anode gases consisting of carbon monoxide and carbon dioxide of the aluminium electrolyzing cells usually small amounts of solid and gaseous fluorides can also be found.

Considerable amount of expediture and efforts have already been devoted to the collection of the gases and to their efficient cleaning from the fluorides detrimental to human health.

The fluoride content of the gas to be cleaned is in the range of 23 to 73 kg/t of aluminium depending on the electrolyzing unit and its capacity. The total separated amount of fluoride fluctuated within the range of 11 to 42 kg/t of aluminium depending on the mode of cleaning and the efficiency of the equipment /Table 5.15/ /154/.

When increasing the capacity of the producing units more and more strict requirements concerning the ervironmental protection have entered into force and at present the fluoride content in the emitted gases must not exceed 1 to 2.5 mg/m^{3} /Table 5.16/. Such a strict requirement can be met economical-

Total Fluoride Losses, and Amount Retrieved from Anode Gases, as Reported for a Number of Aluminium Plants. /All Values are Given in kg F per metric ton of Al produced/

Table 5.15

Plant	Anode type	Total consumption /from material balance/	Collected from the anode gases		
			Total	Particulate	Gas /$HF+CF_4$/
Péchiney Nogueres, France	Söderberg VS	36-38			
Montecatini-Edison, Bolzano, Italy	Söderberg VS	30	18	5	13
Volgogradski, USSR	Söderberg VS	54	27		
USA /Plant I/	Söderberg VS and HS	29			
USSR /Plant I/	Söderberg HS	62	33	9	24
USSR /Plant II/	Söderberg HS	73	42	13	29
USSR /Plant III/	Söderberg HS	30	21		
Dneprovski, USSR	Söderberg HS	28	23.5		
Novokuznetski, USSR	Söderberg HS	23	19.5		
Alusuisse Rheinfelden, Baden, W.Germ.	Both Söderberg and prebaked	33	23		
USA /Pilot plant/	Both Söderberg and prebaked				6-9
Péchiney St.Nikolas, Greece	Prebaked	26-27			
Péchiney St.Jean-de-Maurienne F.	Prebaked	28	13	4	9
Péchiney, France	Prebaked		11-16	5-7	6-9
Montecatini-Edison, Bolzano, Italy	Prebaked	30	15	4	11
Alusuisse Rheinfelden, Baden, W.Germ.	Prebaked	25	18	8	10
Alusuisse Rheinfelden, Baden, W.Germ.	Prebaked	35	20	9	11
Péchiney Bellingham, USA	Prebaked	28			
Ajka, MAT Hungary	Söderberg HS	30	26	8	18
Inota, MAT Hungary	Söderberg VS	32	23	5	18
Tatabánya, MAT Hungary	Söderberg VS	29	18	4	14
Tatabánya, MAT Hungary	Söderberg HS				

Threshold Limit /TLV/ in Different Countries

Table 5.16

Country	Hydrogen fluoride /mg HF/m^3 air at STP/	Total amount of fluoride /mg F/m^3 air at STP/
Great Britain	-	2.2
West Germany	2	-
Netherlands	2	-
U.S.A.	2	2.5
U.S.S.R.	about 0.5	1
Hungary	0.5	1

ly only by the so-called dry gas scrubbing by means of alumina. The gases to be cleaned are conducted through a layer of alumina. The solid and gaseous fluoride compounds become separated and the flucride bearing alumina thus obtained can directly be returned to the production without any after-treatment. In the course of cleaning the chemisorption of HF on the alumir is utilized. At the contact the following phenomena take place:

- diffusion of HF in the vicinity of the alumina particles
- adsorption of HF onto the surface of the particle
- chemical reaction of HF with the alumina.

The efficiency of the chemisorption is influenced by:

- the diffusion velocity of the gas during the period of contact with the alumina
- the average distance between the molecules of the

fluorine gas and the surface of the alumina particle, i.e. the average free space between two alumina particles

- the length of time alumina and stack gases are contacted
- specific surface area of the alumina
- mass of fresh alumina charged.

Both theory and practice indicate that for achieving full chemisorption the adsorbed amount of HF should be less than an entire monomolecular layer, i.e. less than 0.3 mg HF/m^2. Accordingly the entire surface of the alumina should be larger than $3.3 \cdot 10^6$ m^2/kg HF. By this way the minimum specific surface area can be calculated for each amount of alumina by the following relationships:

$$f_{min} = \frac{C \cdot V}{0.3 \cdot M}$$

where: f = required minimum specific surface area, m^2/g
C = fluorine concentration of the gas, mg F/m^3
V = exhausted amount of gas, m^3/h
0.3 = minimum coveredness, mg F/m^2
M = amount of alumina required for cleaning, g/h

or: $$f_{min} = \frac{E_{HF}}{k \cdot M}$$

where: E_{HF} = HF emission kg/t aluminium produced
k = 0.3 mg F/m^2, the minimum coveredness
M = alumina used for cleaning

Considering the relationships the specific surface areas of alumina required for the recovery of the hydrogen fluoride entrained in the anode gases of the Hungarian plants have been calculated /Table 5.17/.

Minimum Surface of Alumina Required for Binding Fluoride Content of the Anode Gases

Table 5.17

	Metal production t/year	HF emission kg F/t Al	Specific alumina consumption t/Al	Alumina surface areas necessary for gas cleaning, m^2/g
Ajka	22200	18.24	1.92	31.7
Inota	32600	17.8	1.93	30.6
Tatabánya	16500	14.2	1.93	24.6

The minimum required specific surface area had also been calculated on the basis of tests carried out on industrial scale. Assuming an emission of 8 kg HF /50 % of the total emission for 1 ton of aluminium produced/ in case of cells with prebaked anodes a minimum specific surface area of 15 m^2/g aluminium had been obtained.

From the point of view of the requirements of the metallurgy the prescription of the specific surface area alone is not enough. In Table 5.18 the properties of alumina simultaneously the requirements of the electrolysis, transportability and dry gas cleaning /scrubbing/ are given.

Quality Requirement of the Metallurgical Process Relating to Alumina Under Various Conditions

Table 5.18

Chemical composition	Characteristic limits	Chemical composition	Characteristic limits
Fe_2O_3	0.02 - 0.03	V_2O_5	0.002 - 0.004
SiO_2	0.015 - 0.025	P_2O_5	0.002 - 0.004
TiO_2	0.006 - 0.010	ZnO	0.015 - 0.025
Na_2O	0.30 - 0.40	CaO	0.04 - 0.06
MnO_2	0.002 - 0.003	MgO	0.002 - 0.005
NiO	0.005 - 0.010	SO_3	0.00? - 0.006
Ga_2O_3	0.006 - 0.012	Cr_2O_3	0.0004-0.0008
		CuO	0.001 - 0.004

Physical properties	Characteristic limits
adh. moisture /300 °C/	0.70-1.00
loss on ignition %	0.50-1.00 /300°C-1000°C/
sieve analysis %	
75-150 micron	20 %
46-75 micron	35 %
- 46 micron	45-50 %
amount of alpha particles, %	55-60 %
angle of repose, a°	35-40
shaken density, kg/l	1.25-1.35
density, g/cm^3	3.5 -3.8
specific surface area, m^2/g	28-35

ANGLE OF REPOSE OF THE ALUMINA

Flowing of the alumina is of importance at the transportation and in the electrolyzing cells from the point of view of heat insulation. This property can be characterized by the angle of repose.

If alumina is poured loose onto a smooth panel it forms a heap /cone/. The angle formed by the alumina cone with the horizontal depends primarily on the size and shape of the alumina particles. The rounder the grains are the smaller the angle of slope and the flatter the cone will be.

According to the investigation of various aluminas the coarse-grained aluminas are characteristic of the smaller angle, while the fine-grained aluminas are characteristic of a larger angle. The cones of the flowing aluminas are limited by a monotonous curve, the limit line of sticky aluminas is zigzagged and the cone of the highly sticky aluminas is already frequently irregular. The angle of repose of the highly flowing aluminas is less than 35°, that of the flowing aluminas is in the range of $35-40^{\circ}$, while that of the sticky aluminas is larger than 40° and that of the highly sticky aluminas exceeds 45°.

For the measurement of the angle of repose a specially developed measuring instrument is used.

The angle of repose expressed in terms of grades is determined by the following formula:

$$R = \text{arc tg } \frac{2H}{D - d}$$

where: H = the height of the alumina cone, i.e. the distance in mm between the base panel and the orifice of the funnel

D = distance in mm, diameter of the alumina cone

d = internal diameter of the orifice of the funnel, in mm

The angle of repose of the various types of aluminas varies in the range of 30 to 60°. The angles of repose of some samples are given in Table 5.12.

DUSTING OF THE ALUMINA

The transportation of the alumina up to the electrolyzing cells is shifted more and more towards the pneumatic transportation. Dusting of alumina at the covering procedure of the cells affects the specific alumina consumption, the air pollution of the pot room, consequently the working conditions. Dust deposit on the bus bars in the shaft hinders their natural cooling and thus influences plant operation.

For the characterization of the dusting of alumina the "falling" and the "carried away" dusting terms are used. When determining the "falling" dusting which occurs if alumina is allowed to fall by gravity is measured, while at the determination of "carried away" dusting, the amount carried away from the falling alumina by the effect of air draft of a given strength is measured.

For the measurement of dusting special instruments are used.

Dusting is in connection with other physico-chemical properties, e.g. grain-size, grain-size distribution, alpha content, angle of repose, compactness, etc. Coarse-grained aluminas in general are less dusting.

DISSOLUTION RATE OF THE ALUMINA

The dissolution of alumina is a function of its surface and crystal structure, thus it requires certain time. The dissolution rate depends on the agitation condition of the material, that is, between dissolution rate under agitated state and without agitation can be differentiated. In the unagitated state the dissolution rate depends on the degree and direction of convection occurring as a consequence of the method of heat transfer. The dissolution depends also on the settling velocity of the grains and connected to this on the shape of the dissolution area. In a flat area the sludge formation can be more advanced, etc. The dissolution tests are carried out in a special equipment developed in the Research Institute for Non-Ferrous Metals.

REFERENCES

/1/ Clement, C.: Rev.Inst.Fr.Petrole 1962, 17, No. 11, p. 1336.
Rev.Inst.Fr.Petrole 1963. 18. No.3, p. 420.

/2/ T.Erdei, G.Schay: Theoretical physical chemistry, Vol. 2. Educational Publishers, Budapest /1954/.

/3/ McBain, J.W., Bakr, A.M.: J.Am.Chem.Soc. 1926. 48, p. 690.

/4/ McBain, J.W., Britton, G.T.: J.Am.Chem.Soc. 1930. 52, p. 2198.

/5/ Rubinstein, A.M., Afanasjev, V.A.: Izv.An. SSSR. Otd. him. 1956. 11. p. 1294.

/6/ Rubinstein, A.M., Kliachko-Gurvich, S.L.: Kinetika i Kataliz, 1962. 39, p. 559.

/7/ Sandstede, G., Robens, E.: Chem.Ing.Techn. 1962. 34, p. 708.

/8/ A Division of North American Aviation Inc. PO. Box. 309. Canoga Park, California, Contraet. AT /11-1/-GEN-8.

/9/ S.Dushman: Fundamentals of the vacuum technique. Publisher of the Hungarian Academy of Sciences /1959/.

/10/ Temkin, M.E.: Zh.Fiz.Himii. 1955. 29, p. 1610.

/11/ Emmet, P.H.: Advances in Colloid Science 1942.

/12/ Cremer, E., Roselius, L.: Angew.Chem. 1958. 70, p. 42.

/13/ Cremer, E.: Angew.Chem. 1959. 71. p. 512.

/14/ Wolf, F., Beyer, H.: Chemische Technik 1959. 11. p. 142.

/15/ Nelsen, F.M., Eggersten, F.T.: Analyt.Chemistry 1958. 30. p. 1387.

/16/ Kiselev, A.V.: Szb.Isledovania v oblasti kromotografii szt. 71. AN. SSSR /1952/.

/17/ Kiselev, A.V.: Sb. Metodi isledovania strukturi visoko-dispersnih i poristih tel. Szt. 111. Izd. AN. SSSR /1953/

/18/ Kiselev, A.V., Sikalova, J.V.: Zav.Lab. 1958. p. 1074.

/19/ Kaunovski, I., Hoffmann, M.: Angew.Chem. 1955. 67. p. 289.

/20/ Marc. R.: Z.Phys.Chem. 1911. 75. p. 710.

/21/ Paneth, F., Vorwerk, W.: Z.Phys.Chem. 1922. 101. p. 480.

/22/ Weiser, H.B., Porter, E.E.: J.phys.Chem. 1927. 31. p. 1824.

/23/ Dubinin, M.N., Zavjeriva, J.D.: Acta Phisicochim. 1936. 4. p. 647.

/24/ J.Mink: Bibliography /Central Physical Research Institute, Budapest/, /1963/.

/25/ A.Imre: Metallurgical Journal, Budapest, 1965. 98. p. 409.

/26/ Paneth, F., Vorwerk, W.: Z.phys.Chem. 1922. 101. p. 445.

/27/ Paneth, F., Thimann, W.: Ber. 1924. 2, p. 1215.

/28/ Hahn, O.: Naturwiss. 1942. 99. p. 147.

/29/ Heckter, M.: Glastechn. Ber. 1934. 12. p. 156.

/30/ Strassmann, F.: Z.Phys.Chem. 1924. 26. p. 353.

/31/ Drake, H., Ritter, G.: Ind.Eng.Chem. 1949. 41. p. 780.

/32/ Barett, C., Joyer, M.: J.Am.Soc. 1940. 62. p. 2839.

/33/ Varren, P.: J.App.Phys. 1949. 20. p. 96.

/34/ Jellinek, I.: Ind.Eng.Chem. 1945. 37. p. 158.

/35/ Fournet, C., Guinier, A.: J.Phys.Radium 1950. 11. p. 516.

/36/ Porod, K.: Kolloid Zeit. 1953. 19. p. 133.

/37/ Garman, V.: Soc.Chem.Ind. 1938. 57. p. 225.

/38/ Dalla, V.: Chem. et Met.Eng. 1938. 45. p. 668.

/39/ Ergun, H.: Anal.Chem. 1951. 23. p. 151.

/40/ Derjagin, A.: J.Appl.Chem. SSSR. 1956. p. 45.

/41/ Calvet, H.: Chem.Abstr. 1949. 47. p. 10985.

/42/ Calvet, H., Astruc, C.: Chem.Abstr. 1949. 47. p. 10949.

/43/ Harkins, D., Jura, G.: J.Am.Chem.Soc. 1944. 66. p. 1362.

/44/ Harkins, D., Jura, G.: J.Phys.Chem. 1943. 11. p. 430.

/45/ Dubinin, M.M.: Fiziko-himicheskie osnovi sorbcionnoi techniki. Izd. 2-e, ONTI /1935/.

/46/ Kistler, S., Fischer, E., Freemann, J.: J.Am.Chem.Soc. 1943. 65. p. 1909.

/47/ Harvey, E.: J.Am.Chem.Soc. 1943. 65. p. 2343.

/48/ Kiselev, A.B.: Usp.him. 1945. 14. p. 367.

/49/ McBain, J.E.: The Sorption of Gases and Vapours by solids. George Routledge and Sons, London /1932/.

/50/ Proc.Roy.Soc. London, A. 120. 59, 80. /1928/.

/51/ Proc.Roy.Soc. London, A. 128. 3, 17. /1930/.

/52/ Kristler, C.: J.Phys.Chem. 1942. 46. p. 1931.

/53/ A.Imre: Mining and Metallurgical Journal.Metallurgy. Budapest, 1970. 103. p. 137.

/54/ A.Imre: Mining and Metallurgical Journal.Metallurgy. Budapest, 1968. 101. p. 338.

/55/ Brunauer, S.: The Adsorption of Gases and Vapours. Princeton, N.J. /USA/, /1945/.

/56/ Lee, C.F., Stross, F.H.: Vortag. 135th. National Meeting Society, Boston, Mass. USA. 9. April /1959/.

/57/ Gregg, S.J.: Oberflächenchemie fester Stoffe. VEB Verlag Technik Berlin /1958/.

/58/ Rootare, H.M., Nyce, A.C.: Internat. Journal of Powder Metallurgy 1971. 1. p. 3.

/59/ Cassidy, H.G., Kun, K.A.: Oxidation-Reduction Polymers: Redox Polymers, New York Wiley-Interscience 1965. p. 155; 167; 307.

/60/ Preeman, H.P., Carol, J.H., Heinly, N.: Agrico and Foot. Chem. 1964. 12. p. 479.

/61/ Everett, D.H., Stone, F.S.: The Structure and Properties of Porous Materials. Butterworth, London /1958/, 10. p. 382.

/62/ Barett, E.P., Joyner, L.G., Halende, P.P.: J.Am.Chem.Soc. 1951. 73. p. 373.

/63/ S.Brunauer, I.Odler: 10th Conference of the Silicate Industry, Budapest. 15-20 June, 1970.

/64/ Ritter, H.L., Drake, L.C.: Ind.Eng.Chem., And.Ed., 1945. 17. p. 782.

/65/ Rossi, G., Usai, G.: Ind.Chin.Ital. 1970. 6. p. 134.

/66/ Ritter, H.L., Erich, L.C.: Anal.Chem. 1948. 20. p. 665.

/67/ Ceaglske, N.H., Hozgen, O.A.: Trans.Am.Inst.Chem.Engrs. 1937. 33. p. 283.

/68/ Z.Szabó, M.Bakos: Contact catalysis. Publisher of the Hungarian Academy of Sciences. Budapest /1966/.

/69/ Balcerzyk, F.: Polimery-Tworzywa Wielkociasteczkowe 1973. 18. p. 173.

/70/ Cserny, S., Smiesek, M.: Chemicke Listy 1962. 56. p. 1296.

/71/ Bárdossy, Gy., Jónás, K., Imre, A., Solymár, K.: Economic Geology 1977. 72. p. 573.

/72/ Imre, A., Baán, I.: Mining and Metallurgical Journal, Budapest, 1968. 101. p. 338.

/73/ Krasotkin, I.S., Kuzmenko, A.S., Abramov, V., Petusok, V.L., Dementev, G.P.: Izv.Vis.Ucheb.Zav.Tsvetnaia Metallurgia, 1973. 1. p. 53.

/74/ Wolfram, E.: Contact wettening. Publisher of the Hungarian Academy of Sciences, Budapest /1971/ p. 10.

/75/ Chessick, J.J., Zettlemoyer, A.C.: Advances in Catalysis and Related Subject. 1959. 11. p. 263.

/76/ Zettlemoyer, A.C.: Hydrophobic Surfaces Academic Press New York, London /1969/ p. 3.

/77/ Reimer, L.: Elektronenmikroskopische Untersuchungsmethoden, Springer, Berlin /1977/.

/78/ Wenk, H.R.: Electronmicroscopy in Mineralogy, Springer, Berlin /1976/.

/79/ Wells, O.C.: Scanning Electron Microscopy, McGraw - Hill Book Co. New York /1974/.

/80/ Reimer, L., Pfefferkorn, G.: Rasterelektronenmikroskopie, Springer, Berlin /1977/.

/81/ Beke, B.: Theory of crushing and comminution. Publisher of the Hungarian Academy of Sciences, Budapest, 1963.

/82/ Tarján, G.: Technique of ore dressing. Educational Publishers, Budapest, 1954.

/83/ Tarján, G.: Mineral dressing. Vol. 1-2. Educational Publishers, Budapest, 1969.

/84/ Taggart, A.F.: Handbook of Mineral Dressing. I.Wiley, New York, 1945.

/85/ Schubert, H.: Aufbereitung fester mineralischer Rohstoffe. I., II., III.
VEB Deutscher Verlag für Grundstoffindustrie. Leipzig, 1967.

/86/ Pethő, Nagy, Schultz, Gy., Tompos, E.: Mineral Dressing, Laboratory Practice. Educational Publishers, Budapest, 1978.

/87/ Werner, G.: Aufbereitungskunde, Band II.
Arbeitsmethoden im Aufbereitungslaboratorium.
Hermann Hübener Verlag. Goslar. 1957.

/88/ Erhard Köster: Granulometrische und morphometrische Messmethoden an Mineralkörnen, Steinen und sonstigen Stoffen. Ferdinand Enke, Stuttgart, 1964.

/89/ Prüfsiebung und Darstellung der Siebanalyse.
SIEBTECHNIK GMBH, Mülheim /Ruhr/. 4. erweiterte und überarbeitete Auflage 1960.

/90/ Lauer, O.: Feinheitsmessungen an technischen Stäuben.
/Leitfaden für den Praktiker./ Herausgeber: ALPINE AG.
Augsburg, 1963.

/91/ Batel, W.: Korngrössenmesstechnik. Springer Verlag 1960.

/92/ Andreasen, A.H.M.: Die Feinheit fester Stoffe und ihre technologische Bedeutung. VDI-Forschungsheft 399., Ausgabe B.Bd. 10. 1939.

/93/ Ba el, W.: Kritische Betrachtunger zur Teilchengrössen-Bestimmung durch Siebanalyse, Windsichten, Sedimentieren, und den Blain-Test. Chem.Ing.Technik, Bd. 31. 1959. Nr. 3. p. 183-191.

/94/ Siebmaschiner zur Durchfürung von Gross-Siebanalysen Aufbereitungstechnik. 1960. Nr. 11. p. 492-493. /Firma Merz, Tiengen/.

/95/ Lauer, O.: Ermittlung der Feinheit und Darstellung der Ergebnisse. ALPINE AG. Augsburg. Sonderdruck. 53.

/96/ Lauer, O.: Korngrössenanalysen mittels Mikropräzisions-sieben. ALPINE AG. Augsbrug. Sonderdruck. 41.

/97/ Lauer, O.: ALPINE Multi-Plex R Zick-zacksichter ein neuer Fliehkraft-Laborwindsichter mit ungewöhnlich weitem Trennbereich. ALPINE AG. Augsburg. Sonderdruck 44.

/98/ Gonell, H.W.: Die Bestimmung der Kornzusammensetzung staubförmiger Stoffe, insbesondere von Zement. Ton-industrie Zeitung, 1929. Nr. 13. Tonindustrie Zeitung, 1935. Nr. 25.

/99/ H. van der Kolk: Mehrjährige Betriebserfahrungen mit dem Bahco-Windsichter. VDI-Berichte. Bd. 7. 1955. p. 25-28.

/100/ D.Bachmann u.H. Gerstenberg: Korngrössenbestimmungen an Kunstoffpulvern. Chem.Ing.Techn. Bd. 29. 1957. Nr. 9. p. 589-594.

/101/ Telle, O.: Ein verbessertes Foto-Sedimentometer. Chem. Ing.Techn. Bd. 26/1954/ Nr. 12. p. 684-686.

/102/ May, J.R.: Particle size measurement with a micromerograph. Mining and Chemical Engineering Review. Vol. 53. 1961. Nr. 12.

/103/ Nassenstein, H.: Automatische Grössenanalyse disperser Systeme durch photoelektrische Abtastung. Chemie Ingenieur Technik. Bd. 27. 1955. Nr. 8/9. und 12.

/104/ Booklets of Casella Electronics Ltd. York.

/105/ Würz, K.: Chemikalien für die Aufbereitung von Mineralien und sonstigen Stoffen.

/106/ Schultz, Gy.: New method of single sedimentation of the decantation grain-size determination. Mining and Metallurgical Journal. /Mining/. Budapest, 1968. No. 10. p. 621-628.

/107/ Lahodny-Sarc, O., Bohor, B.F., Stanek, J. and Hulinsky, V. /1972/ Electronmicroscopy study of bauxites: Proc. 1972. Int. Clay Conf. pp. 781-784.

/108/ Caillére, S. and Pobeguin, Th. /1973/ Sur les particularités du diaspore des bauxites: ICSOBA 3e Cong.Int. Nice, pp. 279-287.

/109/ Bushinsky, G.I. /1975/ Geologia boksitov: Nedra, Moscow, pp. 1-416.

/110/ Zámbó, J. and Solymár, K. /1973/ Prospects of phase transformations in the Bayer process: ICSOBA 3e Cong. Int. Nice, pp. 491-502.

/111/ Ginsberg, H. and Wefers, K.: Aluminium, Enkeverlag, Stuttgart /1962/.

/112/ Árkosi, K.: Hungarian Chemical Journal, Budapest, /1969/ 75. p. 32-43.

/113/ Solymár, K.: /1975/ Evaluation of Sovjet and Hungarian bauxite reference standards from the view in the Bayer cycle. In Mineralogical and Technological Evaluation of Bauxites, pp. 219-226, Budapest.

/114/ Bárdossy, Gy.: Karstic bauxites. Publisher of the Hungarian Academy of Sciences, Budapest. 1977. pp. 165.

/115/ Bárdossy, Gy., Csanády, Á., Csordás, A.: Clays and Clay Minerals 1978. 26. pp. 245-262.

/116/ Dereviankin, V.A., Kuznetsov, S.I., Tcvet.Metal. 34. /1961/46.

/117/ Scott, J.: Extractive Metallurgy of Aluminium, Vol. 1. Interscience, New York /1963/, pp. 203-218.

/118/ Misra, C. and White, E.T.: J. of Crystal Growth, 8. /1971/ p. 172.

/119/ Gynra, B., Jooste, R.F., Brown, N.: J. of Crystal Growth, 21/1974/ p. 141-145.

/120/ Brown, N.: J. of Crystal Growth, 29/1975/ p. 309-315.

/121/ Orbán, M., Csanády, Á., Csordás, A., Kálmán, T.: Scanning microscopic tests at the service of the alumina technology. /Internal subject-matter of the Research Institute for Non-Ferrous Metals, 1978./

/122/ McMillian, R.E., Johnson, G.G.,White, E.W. and Jr.: Computer processing of binary maps of SEM images, SEM Proceedings of the 2nd Annual Scanning Electron Microscopy Symposium, /1969/ pp. 439-445.

/123/ Thaulow, N. and White, E.W.: General method for dispersing and disaggregating partuculate samples for quantitative SEM and optical microscopic studies. Powder Technology 5/1971/72/ pp. 377-379.

/124/ Tarhay, J., Bussem, W.R. White, E.W.: Threedimensional characterization of particles in alumina powders by automated quantitated SEM analysis, 26th Pacific Coast Regional Meeting of the American Ceramic Society /1 Nov. 1973./.

/125/ White, E.W., Görz, H., Johnson, G.G., Lebeedzik J.: Characterization of aluminas by CESEMI, Beiträge der elektronenmikroskopischen Direktabbildung von Oberflächen, 5/1972/ pp. 609-624.

/126/ Wefers, K., Bell, G.: Oxides and Hydroxides of Aluminium. Alcoa Technical Paper No. 19. /1972/

/127/ Réfi Oszkó, I., Várhegyi, Gy, Mándi, T., Gucsi, L.: Chemical Publications, 1972. 38. p. 93-129.

/128/ Mozer, M., Csanády, Á.: VI. Hungarian Electron Microscope Conference, Balatonszéplak, Hungary, 1969.

/129/ Wefers, K.: Erzmetall 17/1964/ p. 583-591.

/130/ Csanády, Á., Várhegyi, Gy., Gémesi, M., Barna, Á., Dömötör, J.: VIII. Hungarian Electron Microscope Conference, Balatonfüred, Hungary, 1973.

/131/ Csanády, Á. Várhegyi, Gy.: Mikroskopie, 29/1973/ p. 57.

/132/ Várhegyi, Gy., Fekete. J., Gémesi, M., Csanády, Á.: VIII. Arbeitstagung "Elektronenmikroskopie" Berlin, /1975/ p. 307.

/133/ Wefers, K.: Zeitschrift für Erzbergbau und Metall hüttenwesen, 20/1967/ pp. 13-19; 71-75.

/134/ Wefers, K.: Berichte der Deutschen Keramischen Gesellschaft, 43/1966/ p. 677-684.

/135/ Orbán, M.: B-III-23/1972 ALUTERV-FKI edition.

/136/ Zámbó, J.: ICSOBA, Jamaica /1977/

/137/ Csanády, Á.: ALUTERV-FKI edition.

/138/ Reiners, E.: The impact crushing mechanism at straight central pushing and the application of this method of loading at crushing. Final report of research. 1962.

/139/ Kézdi, Á.: Soil-mechanical practice. Educational Publishers. Budapest. 1964.

/140/ Gillemot, L.: Material structure and material testing. Educational Publishers. Budapest. 1972.

/141/ Koch, S., Sztrókay, K.: Mineralogy. Vol. 1-2. Educational Publishers. Budapest. 1967.

/142/ Taggart, A.F.: Handbook of Mineral Dressing. I.Wiley, New York 1945.

/143/ ASTM D 409-37.T. Standard Specification /1937/.

/144/ Zeisel, H.G.: Entwicklung eines Verfahrens zur Bestimmung der Mahlbarkeit, Düsseldorf 1952.

/145/ Kannewurf, A.S.: Research pushes grindability guesses into the background. Rock products. /1957/ p. 86-91; 116-118; 121-122.

/146/ Mrákovics, K.: Comparative tests of grindability of bauxites. /Final report of research V-3330/72. Research Institute of the Silicate Industry. Budapest. 1972.

/147/ Schubert, H.: Aufbereitung fester mineralischer Rohstoffe, I., II., III. VEB Deutscher Verlag für Grundstoffindustrie, Leipzig, 1967.

/148/ Rittinger, P.R.: Lehrbuch der Aufbereitungskunde. Berlin, 1867.

/149/ Kirpichov, V.L.: O podobiii pri uprugih iavleniah. Zhurnal Ruskovo fiziko-himicheskovo obchestva. 1874. VI.1. Chasty fizicheskaia, vipusk IX. p. 152-155.

/150/ Kick, F.: Das Gesetz der proportionalen Widerstände Leipzig, 1885.

/151/ Bond, F.C., Wang, J.T.: A New Theory of Comminution. Mining Engineering. /Trans.AIME 187/, 1950. p. 871-878.

/152/ Bond, F.C.: The Third Theory of Comminution. Mining Engineering. /Trans.AIME 193/, 1952. p. 484-494.

/153/ Beke, B.: Course fo grinding procedures and the equilibrium state of the same. Building material. 1962. 13. p. 241-252.

/154/ Zarubezhnaia praktika ochistki gazov ot ftoristih soedinenii pri proizvodstve aluminia. Obzornaia informacija Moszkva, 1974.

/155/ Barillon E.: Avantages at inconvenients au niveau de l'électrolyse at de l'epuration des gaz de cuves, des divers types d'alumine BAYER 4. Intern.Cong.ICSOBA 1978. oct. 9-12.

/156/ Barillon, E., Brantl, T., Magrone, R.: Criteres de qualite de l'alumine pour l'électrolyse at l'épuration des gaz emis 3. Intern. Cong. Nice 1973.

/157/ Menegoz, D.C.: Problémes technologiques pour la filtration des fumees des cuves d'electrolyse

/158/ Mühlrad, Chavineau: Pechiney Prat Daniel dry process for control of fluorine compounds released by aluminium reduction pots AIME Meeting Chicago, februar 1973 Light Metal vol. 1. p. 209.

/159/ Grjotheim, K., Krohn, C., Malinovsky, M., Matiasovsky,K., Thonstad, J.: Aluminium Electrolysis Aluminium - Verlag GmbH. Düsseldorf.

/160/ Solntsev, S.S.: Tsvet. Met. 40. /1967/, p. 59.

/161/ Henry, J.L.: In Extractive Metallurgy of Aluminium Vol. 2. New York 1963. p. 67.

/162/ Menegoz, D.C.: Paper presented at the Third International Congress of ICSOBA, Nice 1973. Sept. 17-21.

/163/ Moser, E.: Erzmetall 22. /1969/, p. 322.